Synthesis of fluorescence labeled scFvs and fluorescent ratiometric detection of antigen

by

Kensuke Yoshikoshi

Submitted to Japan Advanced Institute of Science and Technology
In partial fulfillment of the requirements
For the degree of
Doctor of Philosophy

Supervisor : Professor Dr. Takahiro Hohsaka

School of Materials Science
Japan Advanced Institute of Science and Technology

March 2016

Summary of this research

Bio-based sensors for various target molecules are being used in a wide range of fields. Among them, protein-based fluorescent biosensors are very useful due to high selectivity and sensitivity. However, when the concentration of protein-based fluorescent biosensors is unknown, it is difficult to detect target molecules as fluorescence intensity changes in a quantitative manner. To solve this disadvantage, protein-based fluorescent biosensors that can detect target molecules as fluorescence ratio changes have been developed on the basis of fluorescence resonance energy transfer (FRET). In this research, I developed fluorescent-labeled single-chain antibody variable fragment (scFv) derivatives which enabled us to detect wide range of antigens in ratiometric manner.

In chapter 2, I synthesized double-labeled scFvs having TAMRA and Rhodamine Green at N- and C-termini, respectively, by using non-natural amino acid mutagenesis. For double-labeled scFvs against BGP (bone gla protein) and bisphenol A, fluorescence intensity ratio changes were observed upon the antigen-binding by the combination with FRET and fluorescence quenching. These result suggested that the double-labeled scFvs will be useful for quantitative detection of various target molecules.

In chapter 3, I explored acceptor and donor fluorophore pairs and optimized flexible linker length between the donor fluorophore and the C-terminus of scFvs to improve fluorescence ratio changes. I found that RhodamineRed significantly improved the fluorescence response for anti-bisphenol A scFv. Moreover, I revealed that the use of BODIPYFL-linked amino acid with a shorter linker and a shorter peptide linker at the C-terminus of anti-cMyc and bisphenol A scFvs improved fluorescence ratio change possibly because of decreased undesirable interaction. These findings will be valuable for construction of various double-labeled scFvs and their improvement.

In chapter 4, I incorporated Dansyl group as an environment-sensitive fluorescent probe into scFvs and examined fluorescence spectral properties of Dansyl-labeled scFvs. Four types of Dansyl-labeled scFvs against BGP, bisphenol A, cMyc, and phosphotyrosine showed fluorescence spectral changes upon the antigen-binding, this demonstrates that the environment-sensitive fluorescent probe can be applied to monitor environmental changes around the antigen-binding site and to detect antigens in a ratiometric manner. Dansyl-labeling will become an alternative strategy to design and synthesis of scFv-based fluorescent ratio probes when double-labeled scFv does not show large ratio change upon antigen-binding.

Throughout this study, I successfully developed new fluorescence ratio probes to detect target molecules. Further improvement of the present strategy will enable us to develop

practical diagnostic reagents and cell imaging tools.

Key word : non-natural amino acid mutagenesis, single-chain antibody fragment, FRET and fluorescence quenching, environmental sensitive probe, fluorescence ratiometric detection

Table of contents

1

Background and Overview

1-1 Introduction

Bio-based sensors for various target molecules are being used in a wide range of fields.[1,2] Among them, protein-based biosensors are very useful due to high selectivity and sensitivity. For example, immunoassay using antibodies such as enzyme-linked immunosorbent assay (ELISA) and immunochromatography have been practically used.

The use of fluorescence as a detection method can further improve the sensitivity of protein-based biosensors. Up to now, several detection principles have been applied to biosensors, such as surface plasmon resonance (SPR), mass spectrometry (MS), nuclear magnetic resonace (NMR), and electrochemistry. SPR can detect target molecules by plasmon wave change using biomolecule-immobilized metal surface. Mass spectrometry can directly detect biomolecule complexes with high sensitivity. NMR using stable isotope labels such as ^{19}F has been developed to detect target molecules by chemical shift change. Electrochemistry has also been applied to detect target molecules by electrochemical property change using biomolecule-immobilized electrode. Compared with these detection principles, fluorescence method does not require immobilization of biomolecules unlike SPR and electrochemical methods, and enables us to detect target molecules *in situ*. In addition, fluorescence detection does not need large-size and expensive equipment unlike NMR and MS.

Fluorescent-labeled protein biosensors consist of two components: proteins that can recognize specific ligand molecules, and fluorophores that indicate any fluorescence change upon the binding of ligand molecules. However, when the concentration of protein-based fluorescent biosensors is unknown, it is difficult to detect target molecules as fluorescence intensity changes in a quantitative manner. This is especially problematic under heterogeneous environments such as inside of cells.

To solve this disadvantage, protein-based fluorescent biosensors that can detect target molecules as fluorescence ratio changes have been developed on the basis of fluorescence resonance energy transfer (FRET). This type of fluorescence ratio sensors can quantitatively detect target molecules by measuring fluorescence intensity ratio at two wavelengths without depending on the sensor concentration.

Moreover, this method is useful for fluorescence imaging of living cells. Therefore, protein-based fluorescence ratio biosensors are promising for a wide range of applications.

In the next section, I described various protein-based fluorescence ratio sensors that have been developed up to now.

1-2 Genetically encoded FRET-based protein biosensors

The commonly used FRET-based ratiometric protein biosensors are classified as two groups dependent on the type of fluorescent transducers. The first group is genetically encodable FRET-based biosensors using fluorescent proteins. The second group is biosensors using semisynthetic fluorophores.[3]

The first class of protein biosensors, genetically encoded fluorescent biosensors, have been developed to detect a wide range of molecules.[4] These sensors employ fluorescent proteins such as green fluorescent protein (GFP) derived from marine organisms such as *Aequorea victoria*.[5] A chromophore in GFP is formed by cyclization and oxidation of internal amino acid residues, Ser65-Tyr66-Gly67. Tsien and co-workers developed several GFP variants such as BFP, CFP and YFP by substituting amino acids of and near the fluorophore.[6] Up to now, a variety of colorful fluorescent proteins ranging from blue to red fluorescence emission have been constructed. Some fluorescent proteins emit red fluorescence with excitation at blue light due to large stokes shift.[7]

FRET-based biosensors consist of ligand-binding protein and FRET pair of two different fluorescent protein derivatives at N- and C-termini, respectively. Distance change between the two fluorophores induced by ligand-binding causes FRET change (Figure 1.1). By using this strategy, detection of metal ions, small molecules, enzyme activity, and so on have been achieved.[8,9]

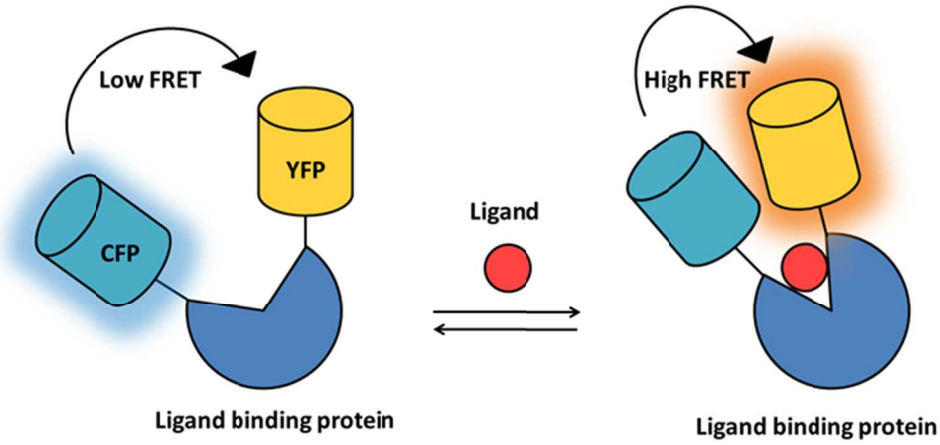

Figure 1.1. Schematic illustration of ratiometric detection of ligand by genetically encoded FRET-based protein biosensor

1-2-1 Improved ratio change of genetically encodable FRET-based protein biosensors

However, there are some issues to be solved for further development of this technique. First issue is the availability of ligand-binding proteins for target molecules. Second issue is that the ligand-binding proteins are required to show large conformational change upon the ligand-binding for FRET efficiency change. Third is the steric hindrance of fluorescent proteins connected with the ligand-binding proteins to the ligand-binding activity. Some bacterial periplasmic-binding proteins exhibit large conformational change upon the ligand-binding and have been applied to FRET protein probes. From these limitations, widely applicable method for construction of FRET protein probes has been desired.

To overcome these limitations, several types of FRET protein probes for detection of target molecules have been developed. Koide and co-workers developed affinity clamping technique (Figure 1.2A), in which a fibronectin type III domain is evolved by phage display to form a complex with a peptide sequence and a natural peptide binding domain.[10] These domains are connected with a short linker. FRET pairs of CyPet and Ypet[11] are fused to N- and C-termini of these domains.[12] Furthermore, Merkx and co-workers developed engineering self-associating ECFP/EYFP pair and adapted these fluorescent proteins to a Zn^{2+} sensor[13]. As a result, new Zn^{2+} sensor showed 6-fold improvement in the dynamic range (Figure 1.2B).[14]

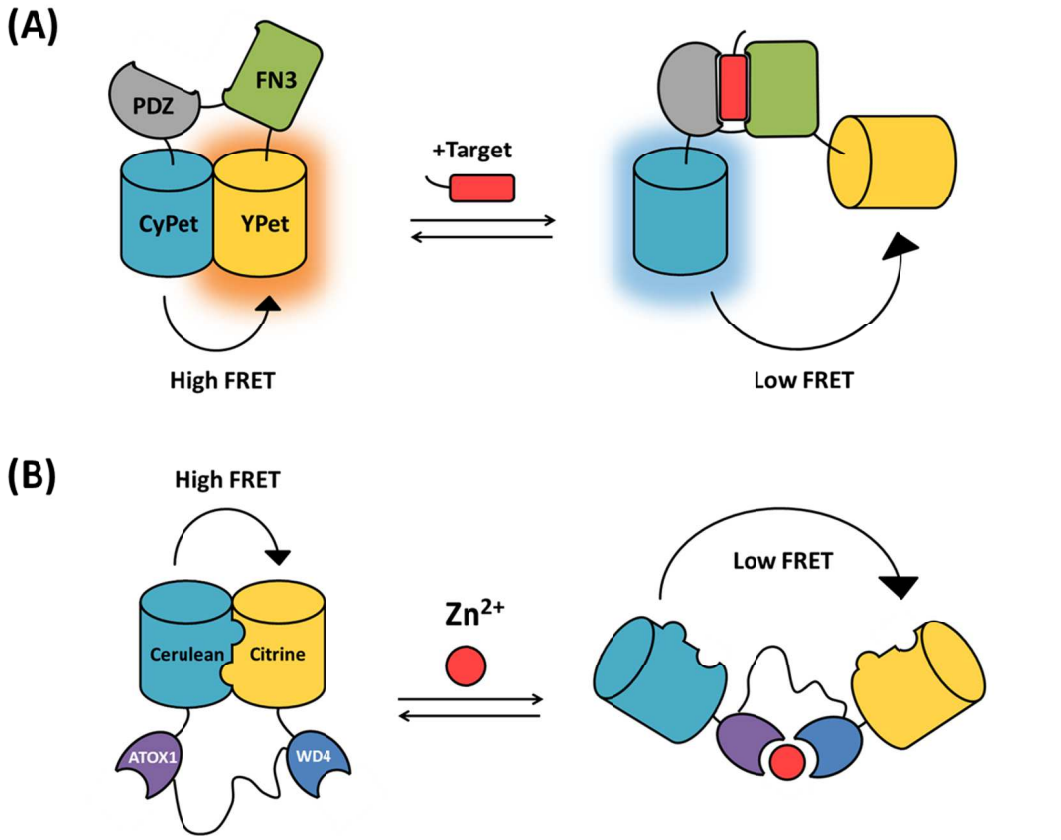

Figure 1.2. (A) Schematic illustration of ratiometric detection of target molecules by the affinity clamping (B) Schematic illustration of ratiometric detection of Zn^{2+} using self-associating ECFP/EYFP pair.

1-2-4 FRET based-antibody biosensors

While the number of ligand binding proteins available in nature is limited, antibodies are available as custom-made ligand-binding proteins with high binding ability and selectivity against various molecules. Fluorophore- and enzyme-labeled antibodies have been used for detection and quantification of antigens as well as cell- and tissue-imaging. However, antibodies labeled by ordinary chemical modification do not exhibit fluorescence intensity change upon the antigen-binding. Therefore, it is usually difficult to detect antigens in a real-time and quantitative manner without washing unbound antibodies. To improve this issue, FRET-based immunoassay has been developed.

Nagamune, Ueda and co-workers developed a method to detect antigens using fluorescent protein-labeled single-chain antibody fragment (scFv) derivatives.[15] Two different fluorescent protein-labeled scFvs bind to different epitopes on human serum albumin (HSA), which induces FRET between the two fluorescent proteins. However, because this method requires two different epitopes on the single antigen, the application of this method is limited.

Next, they developed open-sandwich fluoroimmunoassay (OS-FIA),[16] in which VH or VL fragments are labeled with FRET pairs of fluorescent proteins, respectively. FRET efficiency increases upon the antigen-binding as a result of complex formation of VH, VL, and antigen (Figure 1.3).. Because this method requires one epitope for the antigen detection, the size of antigen is not important. However, because the interaction of the hydrophobic interface between VH and VL may be different depending on the types of scFvs, the application of this method is also limited.

Recently, Ueda and co-workers developed open flower fluoroimmunoassay (OF-FIA),[17] which is composed of a donor-labeled VH and an acceptor-labeled VL. The labeled VH and VL are linked by a disulfide bond. The FRET efficiency changes upon the antigen-binding due to the dimerization of the two fluorescent proteins. However, this method also has a limitation on the size of antigens.

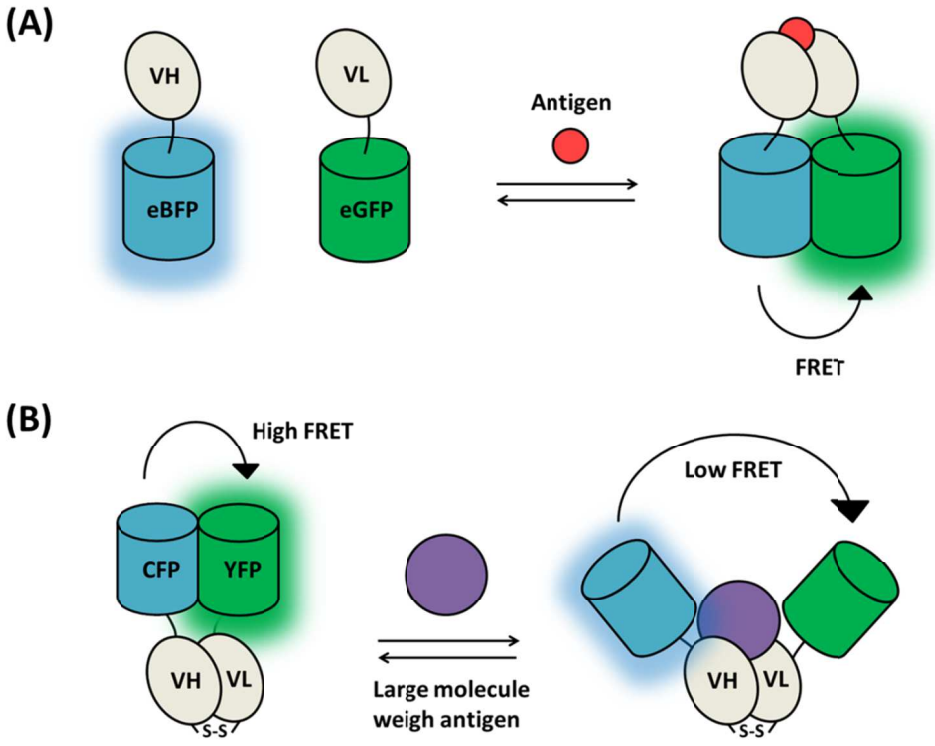

Figure 1.3 (A) Schematic illustration of open sandwich fluoroimmunoassay (OS-FIA). (B) Schematic illustration of open flower fluoroimmunoassay (OF-FIA)

1-3 Semisynthetic fluorescent biosensors

As alternative methods to create protein-based fluorescent biosensors, semisynthetic fluorophore-labeled ligand-binding proteins have been developed as described below.

1-3-1 Environment-sensitive probe-labeled protein biosensors

One of the common semisynthetic fluorescent probes are environment-sensitive probes whose fluorescence intensity or peak wavelength change in accordance with environmental change around the fluorophores. Various fluorescent biosensors have been developed using environment-sensitive fluorophores, in which some show fluorescent ratiometric change upon the ligand binding.

Environment-sensitive fluorophore-labeled amino acid has been employed for facilitation of protein structure and function analysis. Schultz and co-workers synthesized site-specifically environment-sensitive fluorophore-labeled proteins such as myoglobin labeled with L-(7-hydroxycoumarin-4-yl)ethylglycine (HceG),[18] and human superoxide dismutase labeled with 2-amino-3-(5-(dimethylamino)naphthalene-1-sulfonamide)propanoic acid (DansA) [19].

Environment-sensitive probe-labeled amino acids have been applied to detect ligand-binding of proteins. Sisido and co-workers developed streptavidin incorporated with 2-anthrylalanine, γ-(7-methoxycoumarin-4-yl)homoalanine,[20] β-anthra-niloyl-α,β-diaminoprooionic acid,[21] and 2,6-Dansylaminophenylalanine,[22] in which fluorescence quantum yield and peak wavelength were changed upon the binding of biotin.

Schultz and co-workers synthesized glutamine binding protein (QBP) labeled with 3-(6-acetylnaphthalen-2-ylamino)-2-aminopropanoic acid (Anap), which is polar-sensitive fluorophore.[23] This Anap-labeled QBP show fluorescent ratiometric change upon the binding of glutamine. Furthermore, Imperiali and co-worker synthesized M13 peptide labeled with 4-N-,N-dimethylamino-1,8-naphthalimide (4-DMN), 6-N,N-dimethylamino-2,3-naphthalimidoalamine (6-DMN), and other polar-sensitive fluorophores.[24] By using the labeled M13 peptides and calmodulin, concentration of calcium ion can be detected in a ratiometric manner (Figure 1.4). Fluorescent biosensors that show large fluorescent ratio change can be constructed by the incorporation of fluorophores into the positions where environmental change is induced upon the binding of ligands. However, optimization of the incorporation positions of environment-sensitive fluorophores is not so easy.

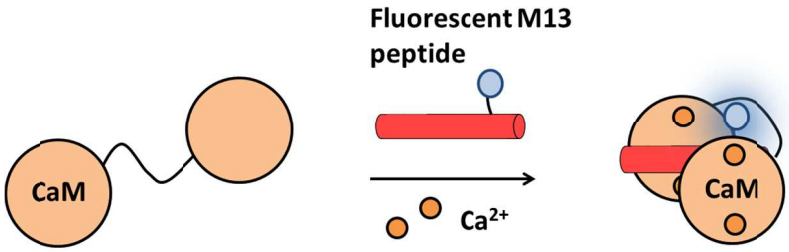

Figure 1.4 Schematic illustration of Ca^{2+} detection by calmodulin and M13 peptide labeled with polar-sensitive fluorescent probes.

1-3-2 Environmental sensitive fluorophore labeled mimick antibody

To detect molecules to which binding proteins are not available, Hahn and co-workers developed fibronectin type III (FN3)-based protein biosensors (Merobody), which were selected from combinatorial libraries and labeled with environment-sensitive probe, merocyanine dye.[25] Src dynamics in cells can be quantified using an SH3-binding Merobody (Figure 1.5). Furthermore, Bedouelle and co-workers developed Ankyrin repeat proteins labeled with N-((2-(oiodoacetoxy)ethyl)-N-methyl)amino-7-nitrobenz-2-oxa-1,3-diazole (IANBD) by using combinatorial libraries.[26]

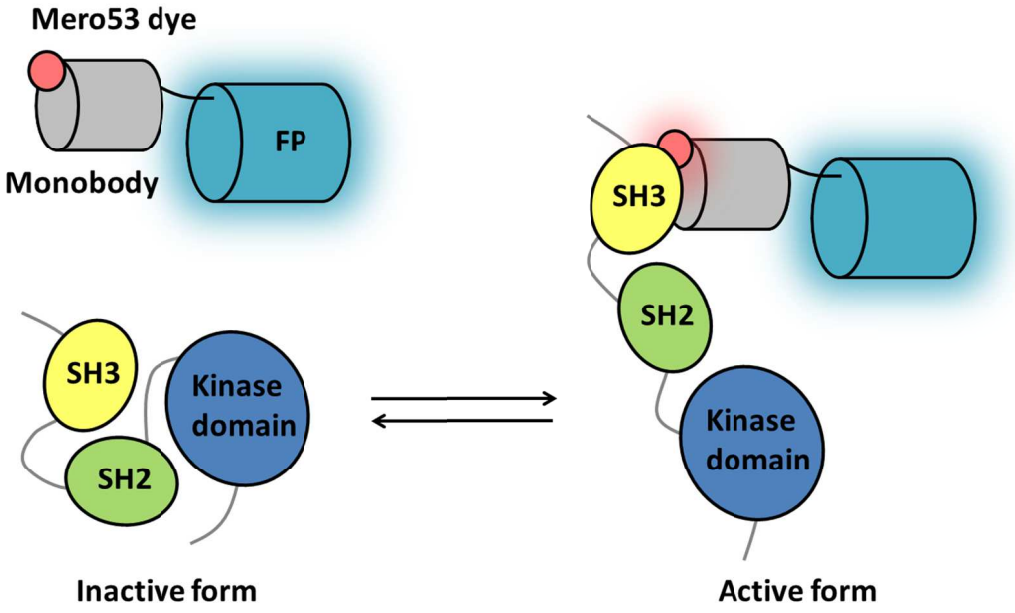

Figure 1.5 Schematic illustration of kinase activity detection by Merobody

1-3-3 Protein-tag-based biosensors

In recent years, Johnsson and co-workers developed new semisynthetic fluorescent ratio sensors, protein-tag-based indicator proteins with fluorescent intramolecular tether (Snifit),[27] which have SNAP-[28] and CLIP-tag[29] proteins. SNAP- and CLIP-tag can be specifically and covalently labeled with O^6-benzylguanine (BG) and O^2-benzylcytosine (BC), respectively. Snifit consists of SNAP-tag, CLIP-tag and a ligand-binding protein. The SNAP-tag moiety was labeled with synthetic molecule containing a fluorophore and an affinity ligand. The CLIP-tag moiety was labeled with another fluorophore that form a FRET pair with the fluorophore linked to the SNAP-tag. Using this strategy, various molecules such as sulfonate groups,[30] glutamate,[31] GABA,[32] and acetylcholine[33] were detected (Figure 1.6). It is advantageous over other methods that Snifit does not require large conformational change of ligand-binding proteins upon the ligand-binding.

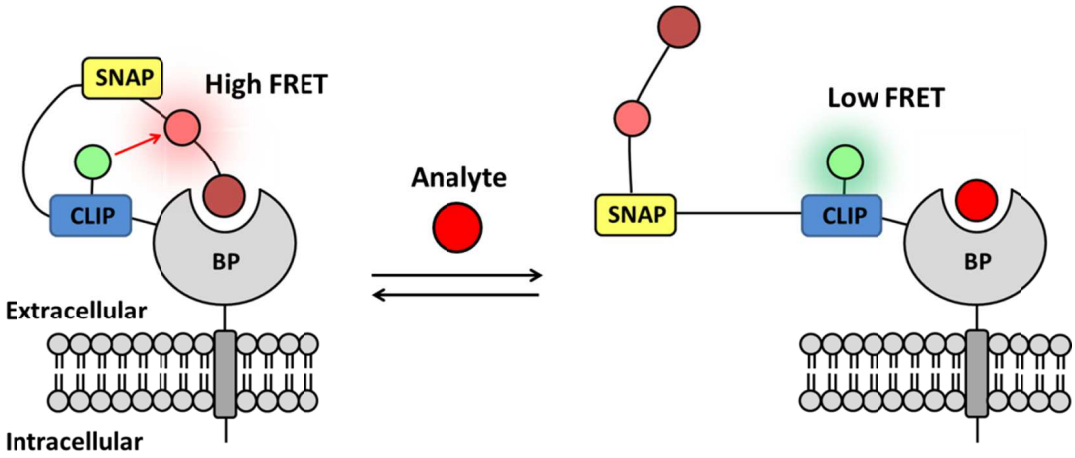

Figure 1.6 Schematic illustration of analyte detection by Snifit.

1-3-4 Ratiometric detection of ligands by combination with FRET and quenching

Hohsaka and co-workers synthesized a double-labeled maltose binding protein by incorporating a FRET donor at the N-terminus and a FRET acceptor at the ligand-binding site (Figure 1.7).[34] The double-labeled maltose-binding protein showed ratiometric fluorescence change upon the maltose-binding by combination with FRET and fluorescence quenching. In the absence of maltose, FRET occurred from the N-terminal donor fluorophore to the acceptor fluorophore incorporated at Tyr210 position, but the acceptor was strongly quenched by Trp residue at the ligand-binding pocket. In the presence of maltose, however, the quenching effect was eliminated and both fluorescences were observed. Furthermore, they reported the ratiometric detection of maltose by combination with bioluminescence resonance energy transfer (BRET) and fluorescence quenching.[35] The combination with FRET and quenching enables ratiometric detection using ligand-binding proteins that does not show large conformational change upon ligand-binding.

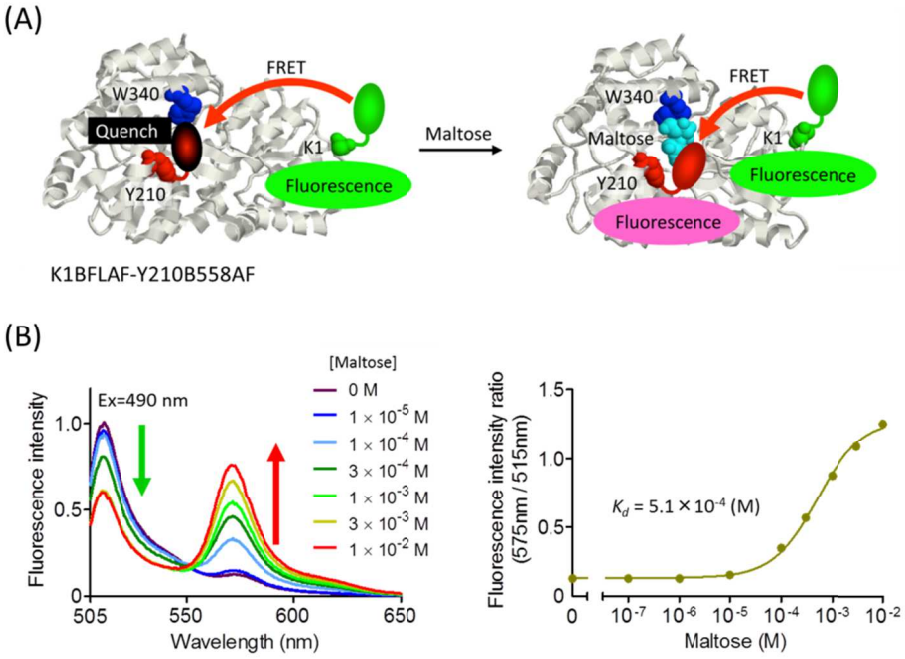

Figure 1.7 (A) Schematic illustration of maltose detection by combination with FRET and fluorescence quenching. (B) Fluorescence spectra of double-labeled maltose-binding protein and titration curve for the fluorescence intensity ratio at 515 nm and 575 nm.

1-4 Incorporation of non-natural amino acids into proteins

Several fluorescent protein biosensors had been synthesized by introducing fluorescent-labeled amino acids into proteins using non-natural amino acid mutagenesis. The nonnatural amino acid mutagenesis is very useful for site-specific fluorescence labeling of proteins and enables to design and synthesis of site-specifically fluorophore-labeled protein based biosensors.[36] In this section, basics and applications of the nonnatural amino acid mutagenesis were described.

1-4-1 Expanded codon-anticodon pairs for non-natural amino acid mutagenesis

The genetic code consists of 64 codons, which encode 20 amino acids and the three termination codons, UAA, UAG and UGA. For site-specific incorporation of non-natural amino acid into proteins, codon and anticodon pairs must be orthogonal to the conventional triplet codons encoding 20 amino acids. Schultz and co-workers[37] and Chamberlin[38] and co-workers assigned amber codon (UAG) to incorporate non-natural amino acids into proteins in a cell-free translation system. In this method, amber suppressor tRNA is chemically aminoacylated with non-natural amino acids to afford aminoacyl-tRNAs, and mRNA containing an amber codon in desired positions is prepared by oligonucleotide-directed mutagenesis. The aminoacyl-tRNA decodes UAG codon and introduces the nonnatural amino acid in a site-specific manner when the aminoacyl-tRNA and mRNA are added to the cell-free translation system. However, competitive decoding of the same codon by the amber suppressor tRNAs and release factor 1 (RF-1) decreased the yield of the protein containing the non-natural amino acid (Figure 1.8).

On the other hand, Sisido and co-workers developed four-base codons and frameshift suppressor tRNAs for the incorporation of non-natural amino acids (Figure 1.8).[39,40] When CGGG codon is recognized by nonnatural aminoacyl-tRNA having CCCG anticodon, a full-length protein that has the non-natural amino acid at the desired position is expressed. On the other hand, when the CGG is recognized by Arg-tRNA having CCG anticodon, the reading frame shifts to +1 and a downstream stop codon terminates the protein synthesis. As a result, a full-length protein containing non-natural amino acid can be obtained. By fusing His-tag at the C-terminus, the full-length protein can be purified using Ni-immobilized materials.

Recently, Schultz and co-workers also reported non-natural amino acid mutagenesis using ochre codon (TAA) in bacteria.[41] In addition, Chin and co-workers reported the incorporation of non-natural amino acids using a quadruplet codon (AAGA) in E. coli.[42]

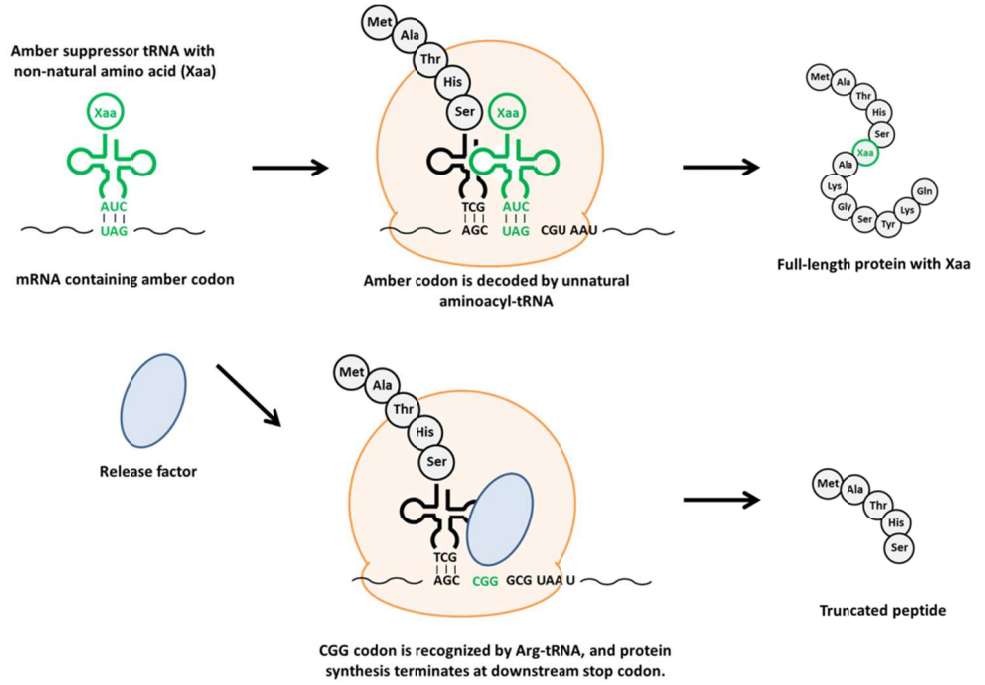

Figure 1.8 Principle of amber suppression method for incorporation of nonnatural amino acids into proteins.

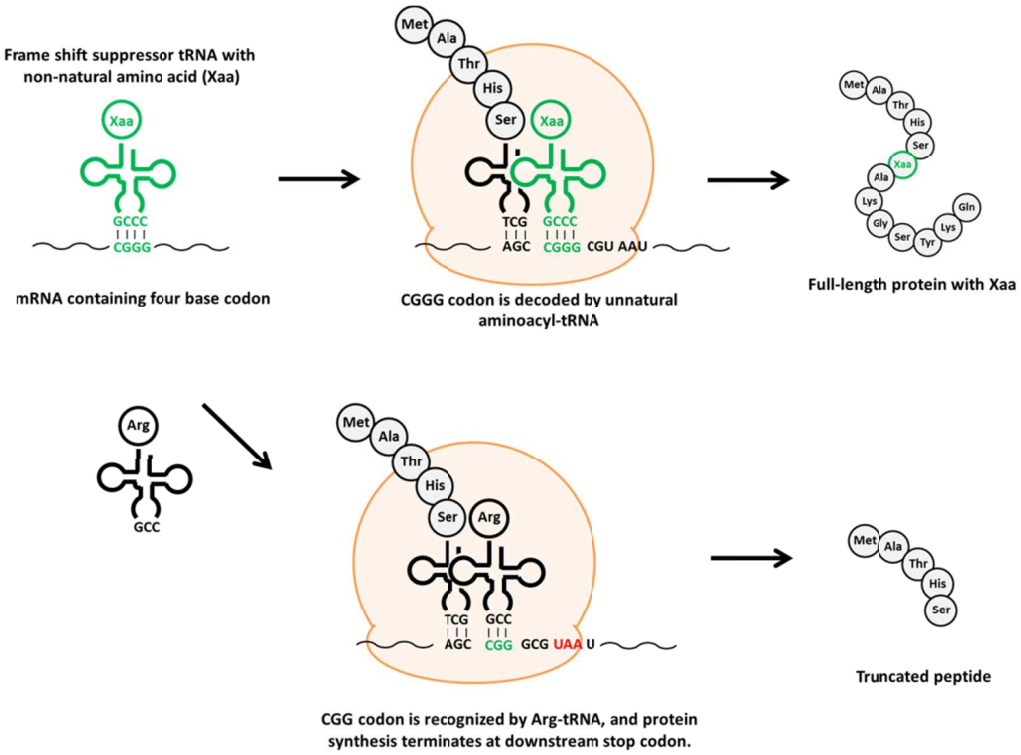

Figure 1.9 Principle of frameshift suppression method for incorporation of nonnatural amino acids into proteins.

Site-specific incorporation of two different non-natural amino acids into different positions of the same protein can be achieved using amber codon and four-base codon in a cell-free translation system.[34,35,43]

Another strategy to expand the genetic code has been proposed by using non-natural base pairs which are orthogonal to natural A-T and G-C pairs such as isocytosine (isoC) and isoguanine (isoG) base pair.[44] Hirao and co-workers developed a pyridine-2-one (y) and 2-amino-6-(2-thienyl) purine (s) pair and revealed that a non-natural codon yAG could be decoded by a tRNA having the corresponding non-natural anticodon CUs.[45] In addition, they developed a Ds-Ps base pair, which is used as substrates for DNA amplification and mRNA transcription, although it has not been applied to the incorporation of non-natural amino acids into proteins.[46]

1-4-2 Aminoacylation of tRNAs with non-natural amino acids

For the incorporation of non-natural amino acids into proteins in vitro, non-natural aminoacyl-tRNA synthesis is required. Hecht and co-workers developed a chemical aminoacylation method in which a chemically synthesized aminoacyl-pCpA is ligated to a truncated tRNA lacking pCpA at the 3'-terminus (tRNA-CA) by T4 RNA ligase (Figure 1.10).[47] Chemically aminoacylated tRNAs obtained by this method enable the incorporation of non-natural amino acids having various side-chains into proteins in cell-free translation systems of E. coli, rabbit reticulocyte,[48] and wheat germ extracts.[49]

On the other hand, Suga and co-workers developed a method to aminoacylate tRNAs using ribozyme (Flexiayme).[50,51] The flexizyme was obtained by the screening of combinatorial pools and by the truncation of the resulting ribozyme. The original flexizyme can charge several amino acids onto tRNAs. The flexiayme system was improved to recognize amino acids activated by 3,5-dinitrobenzyl ester, which enables us to prepare a wide variety of aminoacyl-tRNAs charged with various non-natural amino acids.

Sidido and co-workers developed two strategies for non-enzymatic tRNA aminoacyaltion. First strategy is micellar aminoacylation which employs an amino acid activated ester, a target tRNA, and a cationic detergent, hexadecyltrimethylammonium chloride (CTACI).[52] Second strategy is a peptide nucleic acid (PNA)-assisted aminoacylation in which amino acid activated ester and PNA conjugate is used as a tRNA-recognizing molecule.[53]

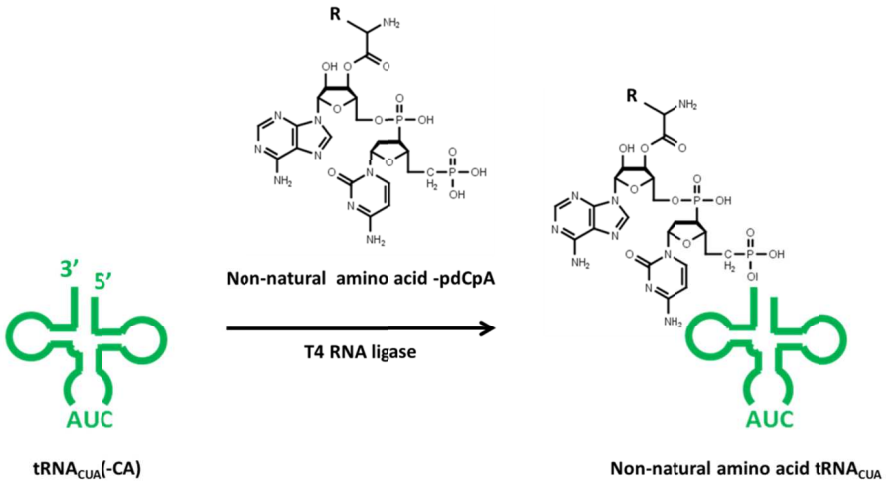

Figure 1.10 Chemical aminoacyaltion of tRNA with a use of T4 RNA ligase.

Schultz and co-workers developed in vivo tRNA aminoacylation method using tyrosyl-tRNA synthetase (MjTyrRS)/tRNA$_{CUA}$ pair derived from *Methanococcus jannaschi*, which was obtained by the selection based on the aminoacylation with a tyrosine-analogous nonnatural amino acids and the orthogonality to E. coli aminoacyl-tRNA synthetase/tRNA pairs.[54] In addition to MjTyrRS, three aminoacyl-tRNA synthetases for nonnatural amino acids have been developed derived from E.coli tyrosyl-tRNA synthesase (EcTyrRS), E coli leucyl-tRNA synthetase (EcLeuRS), and *Methanosarcinae* pyrrolysyl-tRNA synthetase (PylRS).[36]

EcTyrRS/tRNA$_{CUA}$ pair and EcLeuRS/tRNA$_{CUA}$ pair are orthogonal in eukaryotic cells, but not in E. coli, while MjTyrRS/tRNA pair is orthogonal in E. coli but not in eukayotic cells. On the other hand, PylRS/tRNA$_{CUA}$ pair is orthogonal both in bacterial and eukaryotic cells. Using these aminoacyl-tRNA synthetases and tRNA$_{CUA}$ pairs, the synthesis of non-natural amino acid-containing proteins have been achieved in bacteria[23,54-56] and mammalian cells.[57,58]

The choice of tRNAs used for the incorporation of nonnatural amino acids is also essential for efficient incorporation of nonnatural amino acids. Although amber and frameshift suppressor tRNAs can decode amber and four-base codons, endogenous factors such as release factor 1 (RF-1) and triplet tRNAs competitively decode the same codon. As a result, the incorporation of non-natural amino acids into proteins may be inhibited. To improve incorporation efficiency, frameshift suppressor tRNA derived from yeast phenylalanine tRNA[39] and amber suppressor tRNA derived from Mycoplasma capricolum tryptophan tRNA[59] were constructed for efficient incorporation of nonnatural amino acids in E. coli cell-free translation system.

1-4-3 Design of non-natural amino acids

Up to now, the incorporation of a large number of non-natural amino acids into proteins has been reported. For example, non-natural amino acids having biorthogonal functional groups have been used[36,60-62] for large scale synthesis of non-natural amino acid-containing proteins and labeling with functional molecules such as fluorophores.

Hohsaka and co-workers reported the incorporation efficiency of various non-natural amino acids in an E. coli cell-free translation system.[63] They found that the incorporation efficiency of non-natural amino acids is different depending on the side-chain structures, and linearly expanded aromatic side-chains are more favorable for the translation system. According to this finding, fluorescent-labeled *p*-aminophenylalanine derivatives carrying various fluorophores such as BODIPYFL, RhodamineGreen (RhG), and TAMRA (Figure 1.11) were developed for site-specific fluorescence labeling of proteins.[43,64]

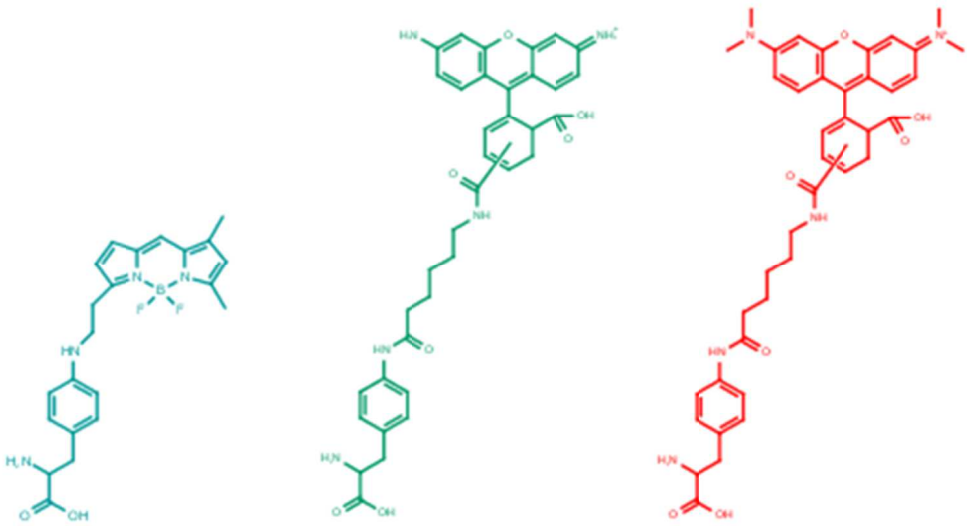

Figure 1.11. Structure of fluorescent nonnatural amino acids that can be incorporated into proteins.

1-5 Content of this thesis

Although various methods have been developed for design and synthesis of protein-based fluorescence ratio probes as described above, general and widely applicable method has never been established. In this doctoral thesis, single-chain antibody-derived fluorescent ratio probes that can detect target molecules as fluorescence ratio change were developed using non-natural amino acid mutagenesis.

Antibodies or single-chain antibody fragments (scFvs) are ideal ligand-binding proteins that can be custom-made against various molecules. Recently, it has been reported that site-specifically fluorescent-labeled scFvs at the N-terminus showed fluorescence enhancement upon the antigen-binding.[65-68] The mechanism of the fluorescence change of the labeled scFvs is proposed as illustrated in Figure 1.12.

In the absence of antigen, the fluorophore at the N-terminus is quenched by tryptophan residues at the hydrophobic interface between VH and VL domains of the scFv. In the presence of antigen, however, the quenching effect is eliminated due to the tight interaction of VH and VL domains, and as consequence, fluorescence intensity increases.

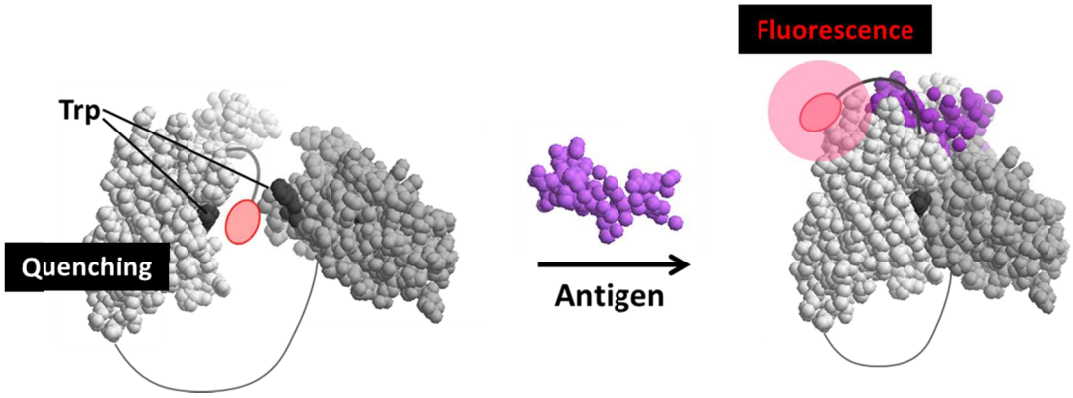

Figure 1.12 Fluorescent-labeled scFv at the N-terminus showing fluorescence intensity change depending on the antigen-binding.

In chapter 2, I described the synthesis of double fluorescent-labeled scFvs and ratiometric detection of antigens by the combination with FRET and fluorescence quenching (Figure 1.13). I incorporated TAMRA-X-AF and RhGreen-X-AF into N- and C-termini of scFvs, in response to four-base codon and amber codon, respectively. I measured fluorescence spectra in the absence and presence of antigens for two types of scFvs.

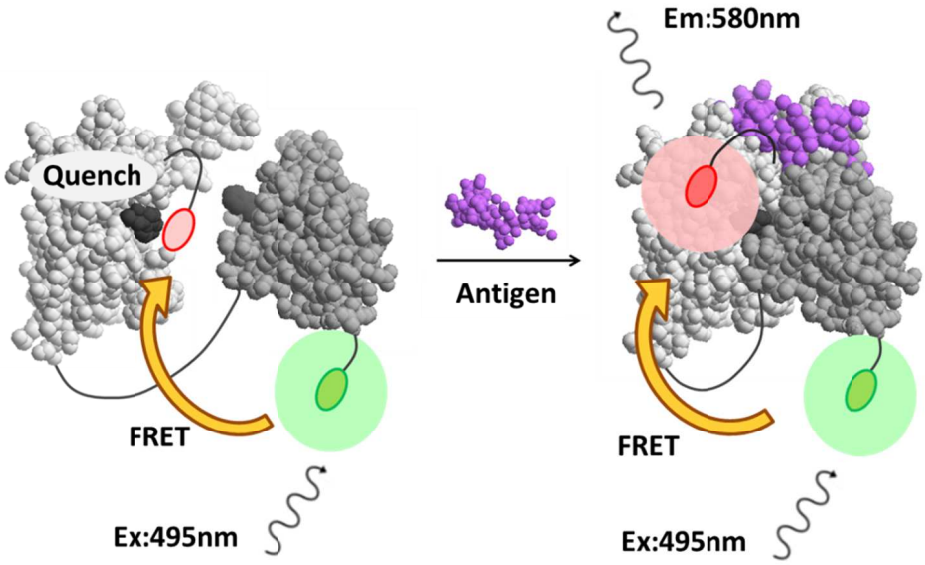

Figure 1.13 Ratiometric detection of antigens using double-labeled scFvs

In chapter 3, I explored new acceptor and donor fluorophore pairs to improve fluorescence intensity ratio change of double-labeled scFvs. I synthesized TAMRA, Rhodamine-Red (RhRed), and TexasRed-labeled scFvs and perform fluorescence measurements to find out suitable fluorophores for each scFv. Next, I investigated the effect of linker length between the donor and the C-terminus of scFvs by using a shorter linker peptide and a fluorescent amino acid with shorter linker.

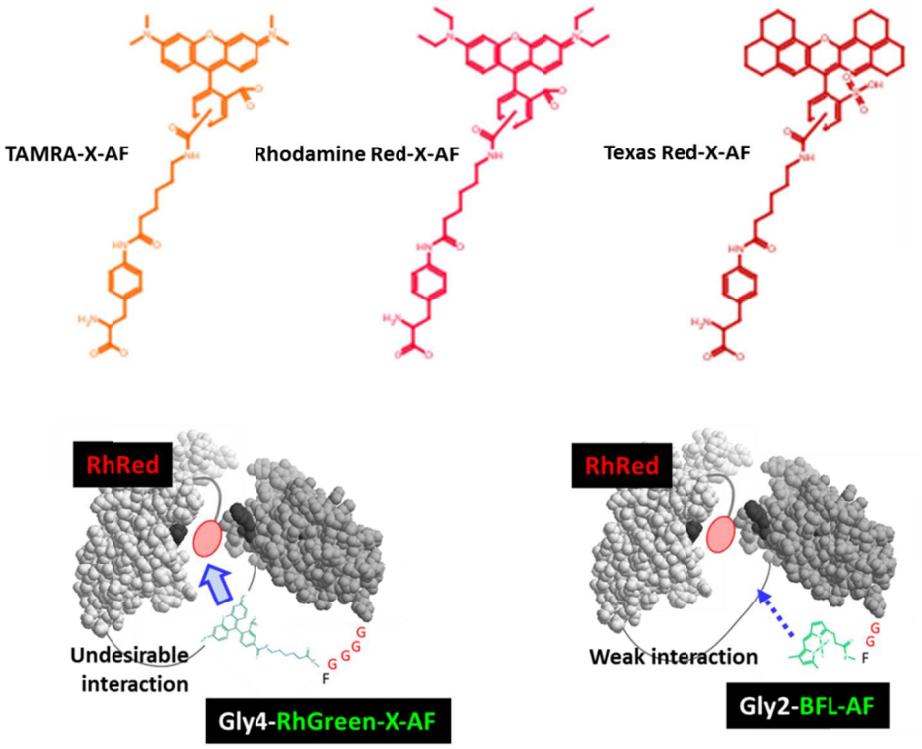

Figure 1.14. Exploring acceptor and donor fluorophore pairs to improve fluorescence ratio changes of double-labeled scFvs.

In chapter 4, I described the synthesis and fluorescence measurement of environment-sensitive fluorophore-labeled scFvs. I used Dansyl group as an environment-sensitive fluorescent probe which exhibits fluorescence intensity and wavelength changes in accordance with the environmental change. Dansyl-linked amino acid was incorporated into four-type of scFvs using amber codon. Fluorescence spectral changes of Dansyl-labeled scFvs upon the antigen-binding were measured for detection of antigens by fluorescence ratio changes.

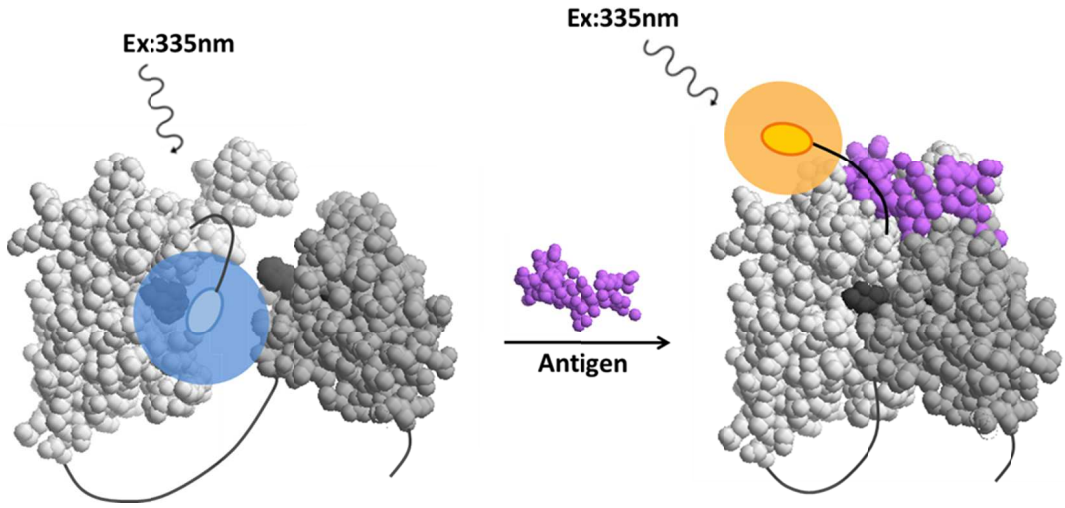

Figure 1.15 Schematic illustration of fluorescence detection of antigen-binding using Dansyl-labeled scFv.

In chapter 5, I summarized this study and described conclusions and future perspectives.

1-5 References

1 W. B. Frommer, M. W. Davidson, R E. Campbell, *Chem Soc Rev.* **2009,** *38, 2833-2841*

2 T. Ozawa, H. Yoshimura, S B. Kim, *Anal Chem.* **2013,** *85, 590-609*

3 T. Tamura, I. Hamachi, *ACS Chem. Biol.* **2014,** *9, 2708-2717*

4 L. Lindenburg, M. Merkx, *Sensors.* **2014***, 14, 11691-11713*

5 M. Chalfile, Y. Tu, G. Euskirchen, W. W. Ward, D. C. Prasher, Science. 1994, 263, 802-805

6 R. Y. Tsien, Angew. *Chem. Int. Ed. Engl.* **2009,** *48, 5612-5626*

7 D. M. Shcherbakova, O. M. Subach, V. V. Verkhusha, *Angewandte. Chemie.* **2010** *51, 10724-10738*

8 A. Miyawaki, *Dev. Cell* **2003**, *4*, 295-305.

9 I. T. Li, E. Pham, K. Truong, *Biotechnol. Lett.* **2006**, *28*, 1971-1982.

10 J. Huang, A. Koide, K. Makade, S. Koide, *Proc. Natl. Acad. Sci. USA,* **2008,** *105, 6578-6583*

11 A. W. Nguyen, P. S. Dauqherty, *Nat Biotechnol.* **2005,** *23, 355-360*

12 J. Huang, S. Koide, *ACS. Chem. Biol.* **2010,** *19, 273-277*

13 D. W. M. Elisabeth, E. H. Toon, D. M. Linda, E. W. Deijer, J. W. Leo, *J. Am. Chem. Soc.* **2007,** *129, 3494-3495*

14 J. L. Vinkenborg, T. J. Nicolson, E. A. Bellomo, M. S. Koay, G. A. Rutter, M. Merkx, *Nature Methods.* **2009,** *6, 737-740*

15 Y. Ohiro, R. Arai, H. Ueda, T. Nagamune, *Anal. Chem.* **2002,** *74, 5786-5792*

16 R. Arai, H. Ueda, K. Tsumoto, W. C.Mahoney, I. Kumagai, T. Nagamune, *Protein Eng.* **2000***, 13, 369-376*

17 C-I. Chung, R. Makino, J. Dong, H. Ueda, *Anal. Chem.* **2015**, *86, 3513-3519*

18 J. Wang, J. Xie, P. G. Schultz, *J. Am. Chem. Soc.* **2006,** *128, 8738-8739*

19 D.Summerer, S. Chem, N. Wu, A. Deiters, J. W. Chin, P. G. Schultz, *Pro. Natl. Acad. Sci. U. S. A.* **2006,** *103, 9785-9789*

20 H. Murakami, T. Hohsaka, Y. Ashizuka. K. Hashimoto, M. Sisido, *Biomacromelecules.* **2000***, 1, 118-125*

21 M. Taki, T. Hohsaka, H. Murakami, K. Taira, M. Sisido, *FEBS Letter.* **2001,** *507, 35-38*

22 T. Hohsaka, N. Muranaka, C. Komiyawa, K. Matsui, S. Takaura, R. Abe, H. Murakami, M. Sisido, *FEBS. Letter.* **2004,** *560, 173-177*

23 H. S. Lee, J. Guo, E. A. Lemke, R. D. Dimla, P. G. Schultz, *J. Am. Chem. Soc.* **2009**, *131, 12921-12923*

24 G. Loving, B. Imperiali, *J. Am. Chem. Soc.* **2008,** *130, 13630-13638*

25 A. Gulyani, E. Vitriol, R. Allen, D. Gremyachinskiy, S. Lewis, B. Dewar, L. M. Graves, B. K. Kay, B. Kuhlman, T. Elston, K. M. Hahn, *Nat. Chem. Biol.* **2011,** *7, 437-444*

26 E. Brient-Litzler, A. Plückthun, H. Bedouelle, *Protein. Eng. Des. Sel.* **2010,** *23, 229-241*

27 M. A. Brun, K-T. Tan, E. Nakata, M. J. Hinner, K. Johnsson, *J. Am. Chem. Soc.* **2009,** *131, 5873-5884*

28 A. Keppler, S. Gendreiziq, T. Gronemeyer, H. Pick, H. Voqel, K. Johnsson, *Nat. Biotechnol.* **2003,** *21, 86-89*

29 G. V. Los, L. P. Encell, M. G. McDouqall, D.D. Hartzell, N. Karassina, C. Zimprich, M. G. Wood, R. Learish, R. F. Ohana, M. Urh, D. Simpson, J. Mendez, K. Zimmerman, P. Otto, G. Viduqiris, J. Zhu, A. Darzins, D. H. Klaubert, R. F. Bulleit, K. V. Wood, *ACS Chem. Biol.* **2008,** *3, 373-382*

30 M. A. Brun, R. Griss, L. Reymond, K-T. Tan, J. Piguet, R. J. R. W. Peter, H. Vogel, K. Johnsson, *J. Am. Chem. Soc.* **2011,** *133, 16235-16242*

31 M. A. Brun, K-T. Tan, R. Griss, A. Kielkowska, L. Reymond, K. Johnsson, *J. Am. Chem. Soc.* **2012,** *134, 7676-7675*

32 A. Masharina, L. Reymond, D. Maurel, K. Umezawa, K. Johnsson, *J. Am. Chem. Soc.* **2012,** *134, 19026-19034*

33 A. Schena, K. Johnsson, *Angew. Chem. Int. Ed.* **2014,** *53, 1302-1305*

34 I. Iijima, T. Hohsaka, *ChemBioChem.* **2009,** *10*, 999-1006.

35 A. Yamaguchi, T. Hohsaka, *Bull. Chem. Soc. Jpn.* **2012,** *85, 576-583*

36 K. Lang, J. W. Chin, *Chem. Rev.* **2014,** *114, 4764-4806*

37 C. J. Noren, S. J. Anthony-Cahill, M. C. Griffith, P. G. Schultz, *Science,* **1989***, 244, 182-188*

38 J. D. Bain, E. S. Diala, C. G. Glable, T. A. Dix, A. R. Chambelin, *J. Am. Chem. Soc.* **1989,** *111, 8013-8014*

39 T. Hohsaka, Y. Ashizuka, H. Murakami, M. Sisido, *J. Am. Chem. Soc.* **1996,** *118, 9778-9779*

40 T. Hohsaka, Y. Ashizuka, H. Taira, H. Murakami, M. Sisido, *Biochemistry,* **2001,** *40, 11060-11064*

41 A. Chatterjee, S. B. Sun, J. L. Furman, H. Xiao, P. G. Schultz, *Biochemistry.* **2013***, 52, 1828-1837*

42 H. Neumann, K. Wang, L. Davis, M,Garcia-Alai, J. W. Chin, *Nature,* **464,** *441-444*

43 D. Kajihara, R. Abe, I. Iijima, C. Komiyama, M. Sisido, T. Hohsaka, *Nature Methods.* **2006***, 3, 923-929*

44 J. D. Bain, C. Switzer, A. R. Chamberilin, S. A. Benner, *Nature.* **1991,** *356, 537-539*

45 I. Hirao, T. Ohtsuki, T. Fujiwara, T. Mitsui, T. Yokogawa, T. Okuni, H. Nakayama, K. Takio, T. Yabuki, T. Kigawa, K. Kodama, T. Yokogawa, K. Nishikawa, S. Yokoyama, *Nat. Biotechnol.* **2002,** *20, 177-182*

46 T. Fujiwara, M. Kimoto, H. Sugiyama, I. Hirao, S. Yokoyama, Bioorg. *Med. Chem. Lett.* **2001,** *11, 2221-2223*

47 T. G. Heckler, L. H. Chang, Y. Zama, T. Naka, M. S. Chorghade, S. M. Hecht, *Biochemistry.* **1984,** *23, 1468-1473*

48 H. Taira, M. Fukushima, T. Hohsaka, M. Sisido, *J. Biosci. Bioeng.* **2005,** *99, 473-476*

49 P. M. England, H. A. Lester, D. A. Dougherty, *Biochemistry.* **1999,** *38, 14409-14415*

50 Y. Bseeho, D. R. Hodgson, H. Suga, *Nat. Biotechnol.* **2002,** *20, 723-728*

51 H. Murakami, H. Saito, H. Suga, *Chem. Biol.* **2003,** *10, 655-662*

52 N. Hashimoto, K. Ninomiya, T. Endo, M. Sisido, *Chem. Commun.* **2005,** *4321-4322*

53 K. Ninomiya, T. Minohata, M. Nishimura, M. Sisido, *J. Am. Chem. Soc.* **2004,** *126, 15984-15989*

54 L. Wang, P. G. Schultz, *Angew. Chem. Int. Ed. Engl.* **2004,** *44, 34-66*

55 J. W. Chin, T. A. Cropp, J. C. Anderson, M. Mukherji, Z. Zhang, P. G. Schultz, *Science,* **2003,** *301, 964-976.*

56 S. M. Hancock, R. Uprety, A. Deiters, J. W. Chin, *J. Am. Chem. Soc.* **2010,** *132, 14819-14824*

57 A. Gautier, D. P. Nguyen, H. Lusic, W. An, A. Deiters, J. W. Chin, *J. Am. Chem. Soc.* **2010,** *132, 4086-4088*

58 A. Chatterjee, J. Guo, H. S. Lee, P. G. Schultz, *J. Am. Chem. Soc.* **2013,** *135, 12540-12543*

59 H. Taira, Y. Matsushita, K. Kojima, K. Shiraga, T. Hohsaka, *Biochem. Biophys. Res. Commun.* **2008,** *374*, 304-308.

60 K. L. Kiick, E. Saxon, D. A. Tirrell, C. R. Bertozzi, *Proc. Natl. Acad. Sci. U.S.A.* **2002,** *99, 19-24*

61 K. Kirshenbaum, S. I. Carrico, D. A. Tirrell, *ChemBioChem.* **2002,** *3, 235-237*

62 D. Datta, P. Wang, I. S. Carrico, S. L. Mayo, D. A. Tirrell, *J. Am. Chem. Soc.* **2002,** *124, 5652-5653*

63 T. Hohsaka, D. Kajihara, Y. Ashizuka, H. Murakami, M. Sisido, *J. Am. Chem. Soc.* **1999,** *121*, 34-40.

64 R. Abe, K. Shiraga, S. Ebisu, H. Takagi, T. Hohsaka, *J. Biosci. Bioeng.* **2010,** *110*, 32-38.

65 R. Abe, H. Ohashi, I. Iijima, M. Ihara, H. Takagi, T. Hohsaka, H. Ueda, *J. Am. Chem. Soc.* **2011,** *133*, 17386-17394.

66 H. J. Jeong, Y. Ohmuro-Masuyama, H. Ohashi, F. Ohsawa, Y. Tatus, M. Inagaki, H. Ueda, *Biosens Bioelectron.* **2013,** *15, 17-23*
67 R. Abe, H. J. Jeong, D. Arakawa, J. H. Dong, H. Ohashi, R. Kaigome, F. Saiki, K. Yamane, H. Takagi, H. Ueda, Sci. Rep. 2014, 4, 4640-
68 H.J. Jeong, H. Ueda, **Sensors.** *2014, 14, 13285-13297*

2

Double fluorescent-labeled single-chain antibodies showing antigen-dependent fluorescence ratio change

2.1 Introduction

Fluorescence-based detection methods for various biomolecules with high specificity and sensitivity are important for elucidation of biological functions and diagnosis of diseases. Among them, fluorescence ratiometric detection enables real-time and quantitative detection of target molecules even if the concentration of probe molecules is unknown. One major strategy for the fluorescence ratio detection is the use of ligand-binding proteins labeled with FRET pairs of two different green fluorescent protein (GFP) derivatives at N- and C-termini, respectively. Distance change between two fluorophores induced by ligand-binding causes FRET change. Based on this strategy, detection of metal ions, small molecules and protein-protein interaction have been achieved.[1,2]

However, there are several limitations for construction of this type of FRET probes. First, natural or engineered ligand-binding proteins for target molecules must be available. Second, distinct conformational change of the ligand-binding proteins upon the ligand-binding is needed to show FRET change. Third, fluorescent proteins fused to the ligand-binding proteins should not disturb the ligand-binding activity. Bacterial periplasmic-binding proteins including maltose-binding protein have been found to exhibit significant conformational change upon the ligand-binding and applied to FRET protein probes.[3,4] However, because of these limitations, general and widely applicable method for design and synthesis of FRET protein probes has never been established.

To overcome these limitations, several types of FRET protein probes for detection of target molecules have been investigated. For example, affinity clamp method[5] and mutually exclusive domain interaction method[6] can induce large distance change between two fluorescent proteins in response to interaction of two ligand-binding domains even through these domains do not exhibit large conformational changes by themselves. SNAP tag and fluorophore-linked ligands were applied to FRET detection of several target molecules through ligand exchange.[7,8] Although these methods do not require large conformational change upon the ligand-binding, specific ligand-binding proteins are still needed. In addition, careful consideration should be given to steric hindrance of large

molecular weight fluorescent proteins and protein tags.

While the number of ligand binding proteins available in nature is limited, antibodies are available as custom-made ligand-binding proteins with high binding ability and selectivity against various molecules. Fluorophore- and enzyme-labeled antibodies have been used for detection and quantification of antigens as well as cell- and tissue-imaging. However, antibodies labeled by ordinary chemical modification do not exhibit fluorescence intensity change upon the antigen-binding. Therefore, it is usually difficult to detect antigens in a real-time and quantitative manner without washing.

It has been revealed that fluorescent-labeled single chain variable fragment (scFv) derivatives exhibit fluorescence intensity change depending on the antigen-binding.[9-12] Fluorescent-labeled scFvs were synthesized by incorporating fluorescent-labeled nonnatural amino acid at the N-terminal region. In the absence of antigen, the fluorophore becomes in close proximity to hydrophobic interface between VH and VL domains and is quenched by conserved Trp residues. This fluorescence quenching is canceled upon the antigen-binding due to tight interaction between VH and VL domains and removal of the fluorophore from the Trp residues. This principle allows to detect various antigens quantitatively.[9] However, fluorescence intensity change at single wavelength is still not enough for precise quantification of antigens in heterogeneous environments like in living cells where antibody concentration is uncertain and changeable.

Here, we reported synthesis of double-labeled scFvs and ratiometric detection of antigens by combination with FRET and antigen-dependent fluorescence quenching. Ratiometric detection can compensate the difference in the concentration of probe molecules and improve the quality of the analysis. Double-labeled scFvs were synthesized by incorporating tetramethylrhodamine (TAMRA) as a FRET acceptor and Rhodamine Green (RhG) as a FRET donor into N-terminus and C-terminus of scFvs, respectively. The site-specific fluorescence labeling can be achieved by nonnatural amino acid mutagenesis using a four-base codon CGGG and an amber codon UAG.[13-15] Double-labeled scFvs detect antigens in a ratiometric manner as follows (Fig 2.1 A): In the absence of antigen, FRET occurs from RhG at the C-terminus to TAMRA at the N-terminus and TAMRA is quenched by Trp residues on hydrophobic interface of the scFv. In the presence of antigen, however, FRET similarly occurs and the quenching of TAMRA is canceled due to tight interaction of V_H and V_L domains. Thereby, fluorescence intensity ratio of TAMRA and RhG (TAMRA/RhG) increases upon the antigen-binding.

We have already synthesized a double-labeled maltose binding protein by incorporating a FRET donor at the N-terminus and a FRET acceptor at the ligand-binding site. The double-labeled protein showed ratiometric fluorescence change upon the ligand-binding by combination with FRET and fluorescence quenching.[14] Application of this principle to antibodies provide a new methodology that enables quantitative detection of any ligands (antigens) as fluorescence ratio change.

2.2 Materials and Methods

Materials

BGP peptide (RRFYGPV), a C-terminal peptide of human osteocalcin (bone gla protein, BGP) was obtained from Genscript (Piscaway, NJ). Bisphenol A (2,2-Bis(4-hydroxyphenyl)propane) was obtained from Tokyo chemical industry (Tokyo, Japan). T4 RNA ligase was obtained from Takara Bio (Otsu, Japan). *E.coli* S30 extract for liner template and MagneHis Ni-particles were obtained from promega (Madison, WI, USA). Zeba desalting column was obtained from Thermo Fisher Scientific (Waltham, MA, USA). Prestained protein marker was obtained from New England Biolabs (Ipswitch, MA, USA).

Preparation of fluorescent aminoacyl-tRNAs.

A yeast phenylalanine tRNA containing a four-base anticodon CCCG and lacking two nucleotides (CA) at the 3' end was prepared by PCR and T7 transcription as described previously.[16] The truncated tRNA was ligated with TAMRA-X-AF-pdCpA[15] in a reaction mixture (90 µL) containing 2.25 nmol of tRNA(-CA), 6.6 nmol of TAMRA-X-AF-pdCpA in DMSO (9 µL), 55 mM HEPES-Na (pH 7.5), 1 mM ATP, 15 mM $MgCl_2$, 3.3 mM DTT, 20 µg/ml BSA, and 108 units of T4 RNA ligase. The reaction mixture was incubated at 4°C for 2 hours. The aminoacylated tRNA was collected by ethanol precipitation. An amber suppressor tRNA derived from *Mycoplasma capricolum* Trp_1 tRNA[17] was prepared and ligated with RhG-X-AF-pdCpA[15] in a similar manner.

Construction of scFv genes.

The N-terminus of scFv genes[9] was fused with Prox-tag[15] containing a four base codon (ATG TCT AAA CAA ATC GAA GTA AAC CGGG TCT AAT GAG). The C-terminus of single-labeled scFvs was fused with GlyGlyGlySer and His tag

sequence. For double-labeled scFv genes, the C-terminus was fused with GlyGlyGlyGly, TAG, and His tag sequence. For C-terminus single-labeled scFvs, the CGGG codon in the N-terminal Prox-tag sequence was replaced by TTT. The scFv genes were amplified by PCR with a forward primer (ATC GAG ATC TCG ATC CCG) and a reverse primer (TAT AGT TCC TCC TTT CAG), and were transcribed to mRNAs using T7 RNA polymerase as described previously.[16]

Cell-free translation.

Fluorescent-labeled scFvs were synthesized in an *E. coli* cell-free translation system.[16] The reaction mixture (60 µL) contained 55 mM HEPES-KOH (pH 7.5), 210 mM GluK, 6.9 mM CH_3COONH_4, 12 mM $(CH_3COO)_2Mg$, 1.2 mM ATP, 0.28 mM GTP, 26 mM phosphoenolpyruvate, 1 mM spermidine, 1.9% PEG-8000, 35 µg/ml^{-1} folinic acid, 0.1 mM 19 amino acids except arginine, 0.01 mM arginine, 2 mM oxidized glutathione, 48 µg of mRNA, 0.9 nmol of TAMRA-X-AF-$tRNA_{CCCG}$ and/or 0.4 nmol of RhG-X-AF-$tRNA_{CUA}$ and 12 µL *E. coli* S30 extract. The reaction mixture was incubated at 37°C for 1 hour. TAMRA-scFvs were synthesized using mRNAs containing CGGG codon at the N-terminal Prox-tag and TAMRA-X-AF-$tRNA_{CCCG}$. RhG-scFvs were synthesized using mRNAs containing UAG at the C-terminal region and RhG-X-AF-$tRNA_{CUA}$. Double-labeled scFvs were synthesized using mRNAs containing both CGGG and UAG codons and both the aminoacyl tRNAs.

After the translation reaction, fluorescent-labeled scFv was purified on Ni-NTA-coated magnetic beads. The translation mixture was diluted by 180 µl of wash buffer (20 mM phosphate buffer, pH 7.5, 0.5 M NaCl, 5 mM imidazole) with 10 M urea and mixed with 24 µL of Ni-NTA beads. After shaking at r.t. for 30 min, beads were washed once with wash buffer, once with wash buffer with 8 M urea, and thrice with wash buffer. Fluorescent-labeled scFv was eluted with elution buffer (20 mM phosphate buffer, pH 7.5, 0.5 M NaCl, 0.5 M imidazole) at r.t. for 30 min with shaking. To remove remaining free fluorophore in the elution solution, gel filtration was performed using Zeba desalting column.

The products before and after purification were analyzed by 10% SDS-PAGE. The gels were visualized by a fluorescence imager (FMBIO-III; Hitachi Software Engineering) with excitation at 488 nm / emission at 520 nm and excitation at 532 nm / emission at 580 nm.

Fluorescence measurement of fluorescent-labeled scFvs.

The purified and gel-filtrated fluorescent-labeled scFv solution (60 μL) was diluted with 450 μL of PBST (20 mM phosphate buffer, pH 7.5, 0.5 M NaCl, 0.05% Tween 20). The resulting solution was divided into 6 tubes (80 μL) and mixed with the serially diluted antigen solutions (20 μL). After incubation at 25°C for 12 hours, fluorescence spectra were measured on Fluorolog-3 (Horiba Jobin-Yvon) at 25°C in a 5×5mm quartz cell. Excitation and emission slit widths were 5.0 nm. For TAMRA-labeled scFvs, fluorescence spectra were measured from 565 nm to 700 nm with excitation at 550 nm. For RhG-labeled and double-labeled scFvs, fluorescence spectra were measured from 510 nm to 700 nm with excitation at 495 nm. Fluorescence intensity ratio of double-labeled scFvs was determined as intensity at 580 nm / intensity at 527 nm. Dissociation constant (K_d) values were calculated by curve-fitting of maximum peak fluorescence intensities or intensity ratios with the use of a sigmoidal dose-response model using GraphPad Prism software (GraphPad, San Diego, CA, USA).

2.3 Results

Synthesis of double-labeled scFvs by incorporation of fluorescent nonnatural amino acids.

The antigen-dependent fluorescence quenching had been demonstrated for several types of scFvs. In particular, scFvs against bone Gla protein (BGP) and bisphenol A showed large fluorescence change,[9] and therefore, was used in this study. The synthetic genes for these scFvs were fused with ProX tag containing CGGG codon at the N-terminus[15] (Fig. 2.1 B). At the C-terminus, four glycine codons and TAG codon were fused together with histidine tag. The tetraglycine sequence was added as a spacer between scFv and Rhodamine Green dye. The scFv genes were amplified by PCR and transcribed to mRNA using T7 RNA polymerase. To decode the CGGG and UAG codons, a frameshift suppressor $tRNA_{CCCG}$ aminoacylated with TAMRA-X-aminophenylalanine (TAMRA-X-AF) and an amber suppressor $tRNA_{CUA}$ aminoacylated with Rhodamine Green-X-AF (RhG-X-AF) were prepared.[15] The scFv mRNAs were expressed in an *E. coli* cell-free translation system in the presence of the fluorescent aminoacyl-tRNAs (Fig. 2.1 B).

The translation products were analyzed by fluorescence imaging of SDS-PAGE (Fig. 2.2). In the co-presence of TAMRA-X-AF-$tRNA_{CCCG}$ and RhG-X-AF-$tRNA_{CUA}$, a full-length anti-BGP scFv showing both red fluorescence of TAMRA and green

fluorescence of RhG was observed. In contrast, a truncated TAMRA-labeled product, whose mobility was slightly faster than the double-labeled scFv, was observed only in presence of TAMRA-X-AF-tRNA$_{CCCG}$. In the presence of RhG-X-AF-tRNA$_{CUA}$, no band was observed due to unsuccessful decoding of the CGGG codon at the N-terminus. These results indicated that the double-labeled anti-BGP scFv containing TAMRA-X-AF and RhG-X-AF at the N- and C-termini, respectively, was successfully synthesized in the co-presence of the two fluorescent aminoacyl-tRNAs. As controls, single-labeled scFvs containing either TAMRA-X-AF or RhG-X-AF were also prepared from the corresponding mutant scFv genes. Fluorescent SDS-PAGE analysis indicated the successful synthesis of the single-labeled scFvs (Fig. 2.2).

The double- and single-labeled scFvs having His tag at the C-terminus were purified by Ni-NTA beads, followed by gel filtration to remove remaining trace amount of free fluorescent amino acids (Fig 2.3). Double- and single-labeled anti-bisphenol A scFvs were also synthesized and purified in a similar manner.

Fluorescence measurement of anti-BGP scFvs.

Fluorescence spectra of the single- and double-labeled anti-BGP scFvs were measured in the presence of various concentrations of BGP peptide (Fig. 2.4). Single-labeled anti-BGP scFv with N-terminal TAMRA showed increase in fluorescence intensity increased to 6.7-fold upon the binding of BGP (Fig. 2.4A). The dissociation constant (K_d) was determined to be 6.3×10^{-9} M by fitting the binding curve. These values were identical to those obtained in the previous report.[9] The single-labeled scFv with C-terminal RhG, on the other hand, showed nearly constant fluorescence regardless of the addition of the antigen (Fig. 2.4B). This suggests the antigen-dependent quenching of RhG at the C-terminus is much lower than the N-terminal TAMRA, possibly due to different location of the fluorophores. This property is suitable for FRET

Fluorescence spectra of the double-labeled anti-BGP scFv were measured with excitation at 495 nm and 550 nm. In case of excitation at 495nm, both RhG and TAMRA fluorescence was observed (Fig. 2.4C), indicating FRET from RhG to TAMRA. The fluorescence intensity of TAMRA significantly increased upon the addition of BGP peptide, while RhG showed nearly constant fluorescence (Fig. 2.5C). This observation is explained as follows: In the absence of antigen, FRET occurred from RhG to TAMRA but TAMRA was quenched by Trp residues. The binding of the antigen canceled the quenching of TAMRA although FRET efficiency was nearly constant.

The fluorescence intensity ratio of TAMRA and RhG (TAMRA/RhG) increased to 3.8-fold. The K_d value was determined by fitting the intensity ratio change to be 6.1×10^{-9} M. The good agreement of the K_d values for double- and single-labeled scFv suggests that the ratio change was caused by the antigen-binding and that RhG at the C-terminus did not affect the binding activity of the double-labeled scFv.

In case of excitation at 550 nm, fluorescence intensity of TAMRA increased to 5.6-fold upon the antigen-binding (Fig. 2.4D). This increase was a little lower than that of the single-labeled scFv, possibly due to that RhG at the C-terminus may interact with TAMRA in the presence of the antigen and decrease the TAMRA fluorescence to some extent.

Fluorescence measurement of anti-bisphenol A scFvs.

Fluorescence changes of double- and single-labeled anti-bisphenol A scFvs (Fig. 2.5) were measured in a similar manner. Single-labeled scFv with TAMRA at the N-terminus showed increase in fluorescence intensity to 1.6 fold upon the addition of bisphenol A (Fig. 2.5A). The K_d value was determined to be 1.4×10^{-9} M. These values were almost the same as previously obtained ones.[9] On the other hand, fluorescence intensity of single-labeled scFv with RhG at the C-terminus was constant (Fig. 2.5B), suggesting that RhG at the C-terminus does not. Double-labeled scFv showed slight decrease in RhG fluorescence and moderate increase in TAMRA fluorescence upon the antigen-binding (Fig. 2.5C). As results of these changes, fluorescence ratio increased to 1.3-fold. The K_d value (5.5×10^{-9} M) was comparable to that of single-labeled TAMRA-scFv, suggesting that RhG at the C-terminus did not influence the binding activity of the anti-bisphenol A scFv as in the case of the anti-BGP scFv. Under the excitation at 550 nm for the double-labeled scFv, fluorescence intensity increased to 1.2-fold (Fig. 2.5D). The lower fluorescence change than the single-labeled TAMRA-scFv may be because of the interaction between TAMRA and RhG as in the case of the anti-BGP scFv.

2.4 Discussion

In both the double-labeled scFvs, fluorescence intensity of RhG (donor) was nearly constant regardless of the antigen concentration. This suggests that FRET efficiency is insensitive to the antigen-binding and that the average distance between donor and acceptor is nearly constant. Although the three-dimensional structures of the antibodies used here are not available, structures of anti-cMyc tag antibody with and without antigen[18] were referred on the basis of the similarity of antibody structures. The structural data of anti-cMyc antibody indicates the Cα-Cα distances between the N-terminus of VH domain and the C-terminus of VL domain are 35.8 Å and 36.2 Å in the absence and presence of the antigen, respectively. These values suggests that the average distance between N-terminal TAMRA and C-terminal RhG is not altered upon the antigen-binding. Moreover, these distances are smaller than R_0 value for the RhG and TAMRA pair, which is calculated to be 61 Å under the assumption that the orientation factor is 2/3. This suggests that FRET may efficiently occur even if the linkers between the fluorophores and the amino acid main chain are fully extended.

In most FRET protein probes developed previously, distance change between donor and acceptor is essential for FRET change. Our present system utilizing FRET and fluorescence quenching does not require such distance change. This unique feature makes it easy to apply this concept to other proteins including antibodies which show ligand-dependent fluorescence quenching without changing the conformation upon the ligand-binding.

The change in fluorescence intensity ratio of the double-labeled anti-BGP scFv (3.8-fold) was significantly high compared with typical FRET protein probes. On the other hand, the double-labeled anti-bisphenol A showed 1.3-fold. This difference is due to the difference in the fluorescence response of single TAMRA-labeled scFvs. For further improvement of the fluorescence ratio change, it will be needed to improve fluorescence response of single-labeled scFvs and derivatize them into double-labeled ones. In addition, unfavorable interaction between RhG at the C-terminus and TAMRA at the N-terminus observed here should be avoided by modifying the position of the fluorophores and linker structures.

2.5 Conclusion

We developed double-labeled scFvs showing antigen-dependent fluorescence ratio change. Site-specific double fluorescence labeling of scFvs was achieved by the incorporation of TAMRA and RhG using nonnatural amino acid mutagenesis technique. The fluorescence ratio change is based on combination with FRET and antigen-dependent fluorescence quenching, and therefore, can be available universally for various antigen-antibody pairs.

In recent years, fluorescent protein probes based on antibodies and antibody mimics allowing ratiometric antigen detection have been reported.[19-21] The present method has several advantages over previous methods. First, double-labeled antibodies showing fluorescence ratio change can be easily obtained from single-labeled antibodies showing antigen-dependent fluorescence intensity change. Second, the use of small fluorescent nonnatural amino acids can avoid steric hindrance derived from large fluorescent proteins. Third, the cell-free expression system allows simple and rapid preparation of the double-labeled scFvs. Although the low productivity of the cell-free expression is disadvantageous, highly sensitive fluorescence analytical methods can compensate for this drawback.

The double-labeled scFvs will be useful for various applications such as diagnostic analysis and fluorescence ratio imaging. It has been reported that some scFvs maintained the antigen-binding activity in intracellular environment.[22,23] Fluorescence ratio imaging of double-labeled scFvs in living cells will become a powerful method for quantitative localization analysis of desired molecules.

References

1 A. Miyawaki, *Dev. Cell* **2003**, *4*, 295-305.

2 I. T. Li, E. Pham, K. Truong, *Biotechnol. Lett.* **2006**, *28*, 1971-1982.

3 M. D. Dwyer, H. W. Hellinga, *Curr. Opin. Struc. Biol,* **2004,** *14*, 495-504.

4 I. L. Medintz, J. R. Deschamps, *Curr. Opin. Biotechnol.* **2006,** *17*, 17-27.

5 L. Lindenburg, M. Metkx, S*ensors.* **2014,** *14*, 11691-11713.

6 J. Hunang, S. Koide, *ACS Chem. Biol.* **2010,** *5*, 273-277.

7 G. Lukinavicius, K. Johnsson, *Curr. Opin. Chem. Biol.* **2011,** *15*, 768-774.

8 M. A. Brun, K-T. Tan, E. Nakata, M. J. Hinner, K. Johnsson, *J. Am. Chem. Soc.* **2009,** *131*, 5873-5884.

9 R. Abe, H. Ohashi, I. Iijima, M. Ihara, H. Takagi, T. Hohsaka, H. Ueda, *J. Am. Chem. Soc.* **2011,** *133*, 17386-17394.

10 H. J. Jeong, Y. Ohmuro-Matsuyama, H. Ohashi, F. Ohsawa, Y. Tatsu, M. Inagaki, H. Ueda, *Biosens.Bioelectron.* **2013,** *40*, 17-23.

11 R. Abe, H. J. Jeong, D. Arakawa, J. H. Dong, H. Ohashi, R. Kaigome, F. Saiki, K. Yamane, H. Takagi, H. Ueda, *Sci. Rep.* **2014,** *4*, 4640.

12 H. J. Jeong, H. Ueda, *Sensors.* **2014,** *14*, 13285-13297.

13 D. Kajihara, R. Abe, I. Iijima, C. Komiyama, M. Sisido, T. Hohsaka, *Nat. Methods* **2006**, *3*, 923-929.

14 I. Iijima, T. Hohsaka, *ChemBioChem.* **2009,** *10*, 999-1006.

15 R. Abe, K. Shiraga, S. Ebisu, H. Takagi, T. Hohsaka, *J. Biosci. Bioeng.* **2010,** *110*, 32-38.

16 T. Hohsaka, D. Kajihara, Y. Ashizuka, H. Murakami, M. Sisido, *J. Am. Chem. Soc.* **1999,** *121*, 34-40.

17 H. Taira, Y. Matsushita, K. Kojima, K. Shiraga, T. Hohsaka, *Biochem. Biophys. Res. Commun.* **2008,** *374*, 304-308.

18 N. Krauss, H. Wessner, K. Welfle, H. Welfle, C. Scholz, M. Seifert, K. Zubow, J. Aÿ, M. Hahn, P. Scheerer, A. Skerra, W. Höhne, *Proteins* **2008**, *73*, 552-565.

19 A. Gulyani, E. Vitriol, R. Allen, J. Wu, D. Gremyachinsky, S. Lewis, B. Dewar, L. M. Graves, B. K. Kay, B. Kuhlman, T. Elston, K. M. Hahn, *Nat. Chem. Biol.* **2011,** *7*, 437-444.

20 H. Ueda, J. Dong, *Biochimica et Biophysica Acta.* **2014***, 1844*,1951-1959.

21 C. I. Chung, R. Makino, J. Dong, H. Ueda, *Anal. Chem.* **2015,** *87*, 3513–3519.

22 S. M. Lynch, C. Zhou, A. Messer, *J. Mol. Biol.* **2008***, 377*, 136–147.

23 N. E. Weisser, J. C. Hall, *Biotechnol. Adv.* **2009,** *27*, 502-520.

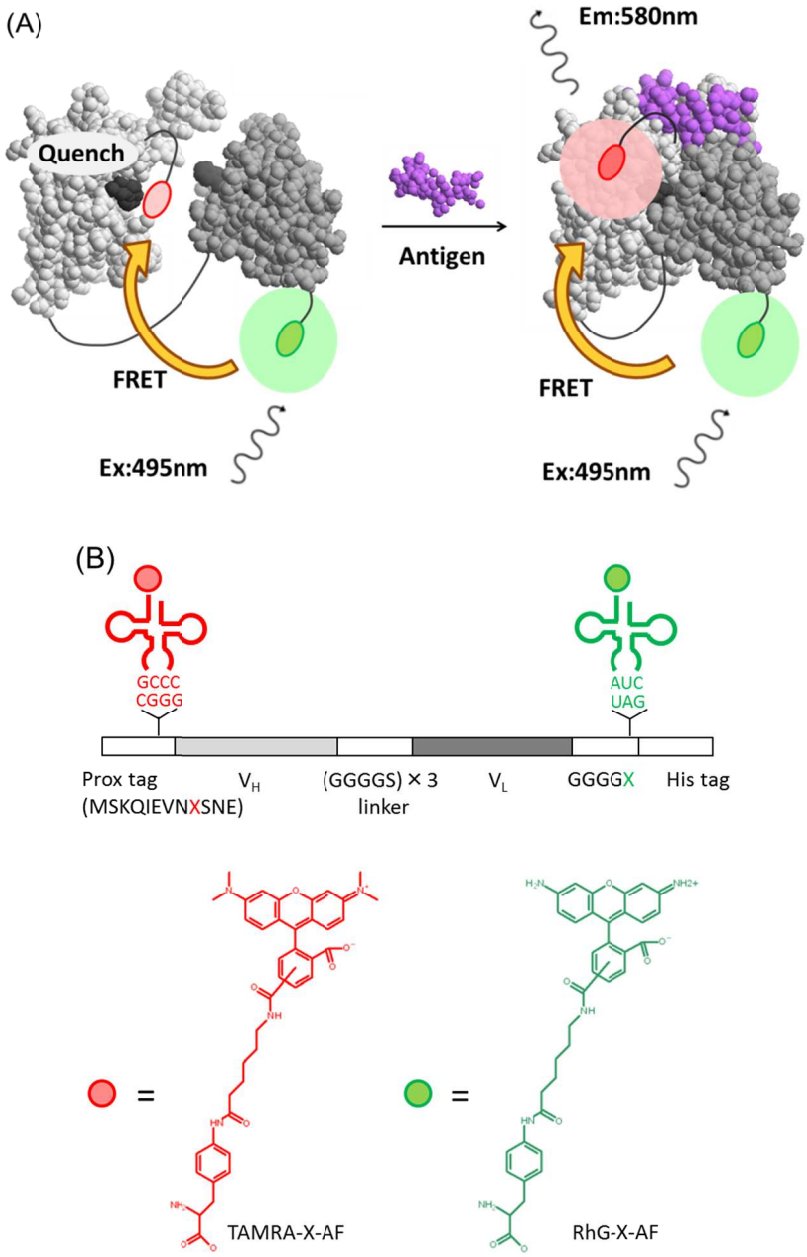

Figure 2.1 (A) Schematic illustration of fluorescence ratio detection of antigen-binding by combination with FRET and fluorescence quenching. (B) Schematic illustration of synthesis of double-labeled scFv using a four-base codon (CGGG) and amber codon (UAG) in a cell-free translation system.

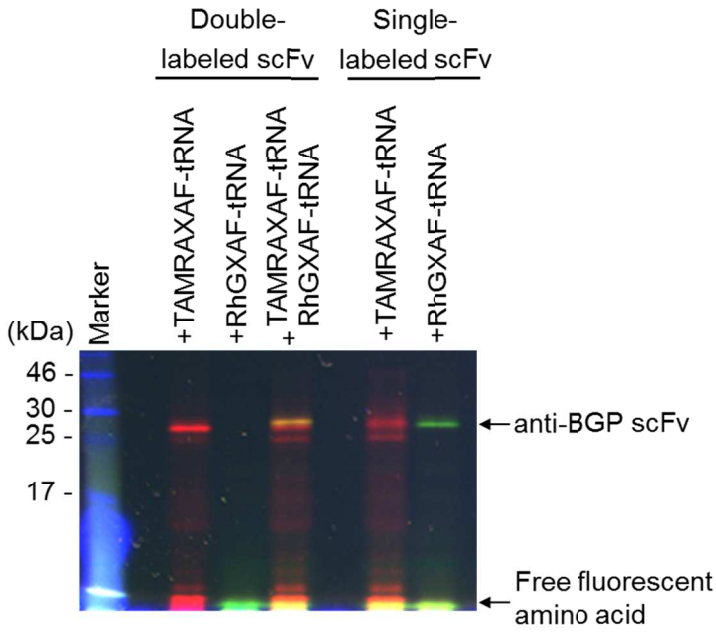

Figure 2.2 Fluorescence image of SDS-PAGE for the expression of double-labeled anti-BGP scFv in the presence of TAMRA-X-AF-tRNA$_{CCCG}$ and RhG-X-AF-tRNA$_{CUA}$ in a cell-free translation system. Single-labeled anti-BGP scFv with TAMRA at the N-terminus and that labeled with RhG at the C-terminus were also expressed.

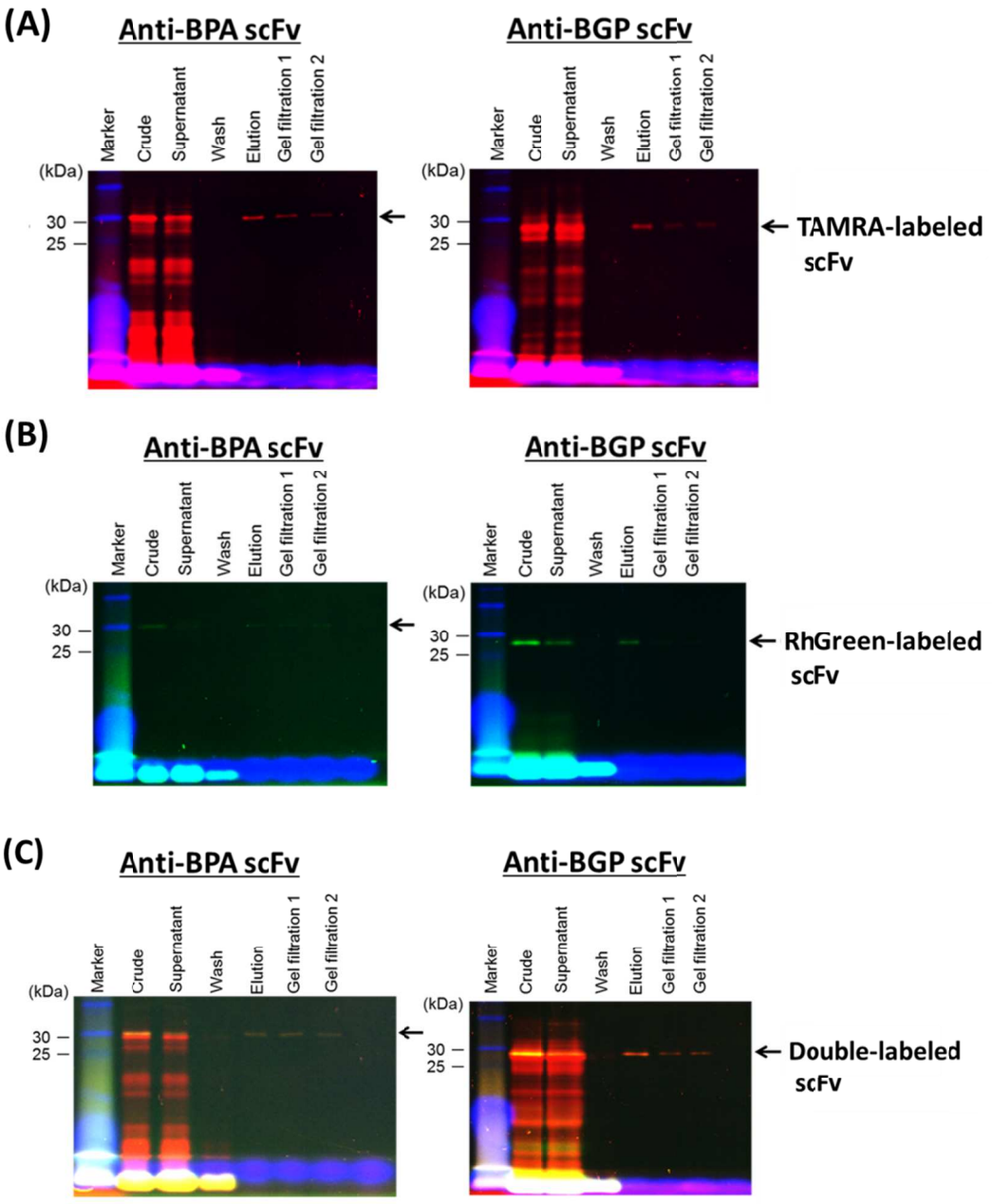

Figure 2.3 Fluorescence imaging of SDS-PAGE for purification of fluorescent-labeled scFvs. (A) Purification of TAMRA-labeled anti-bisphenol A (BPA) and BGP scFvs. (B) Purification of RhGreen-labeled anti- bisphenol A (BPA) and BGP scFvs. (C) Purification of Double-labeled anti- bisphenol A (BPA) and BGP scFvs.

(A) TAMRA-labeled anti-BGP scFv

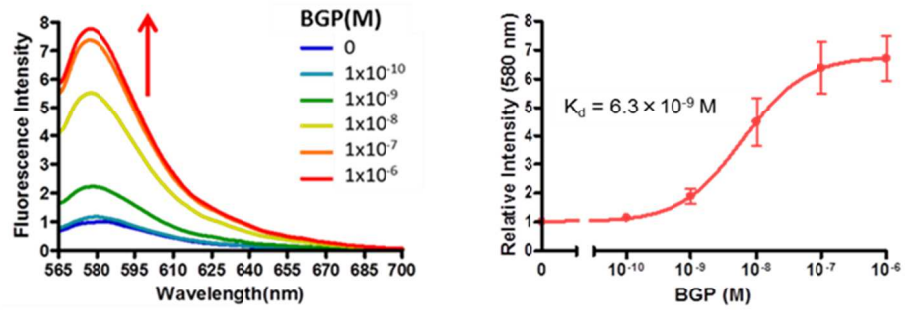

(B) RhG-labeled anti-BGP scFv

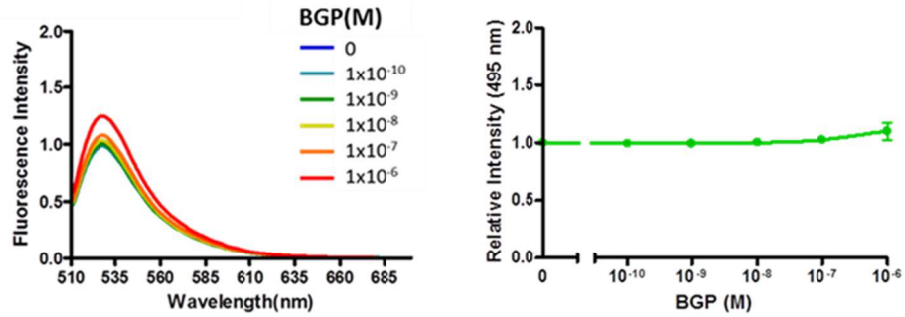

(C) Double-labeled anti-BGP scFv (Ex 495 nm)

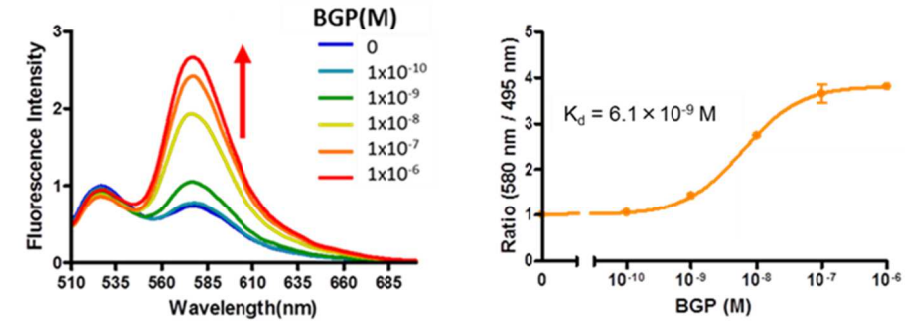

(D) Double-labeled anti-BGP scFv (Ex 550 nm)

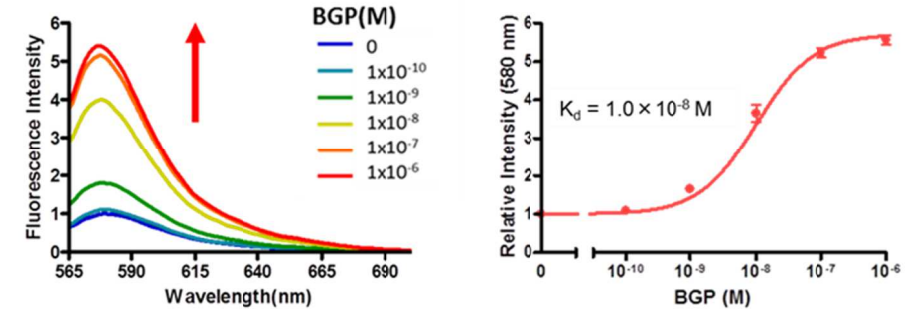

Figure 2.4 Fluorescence measurement of fluorescent-labeled anti-BGP scFvs. (A) Fluorescence spectra of TAMRA-labeled anti-BGP scFv with excitation at 550 nm in the presence and absence of BGP peptide, and titration curve for the fluorescence intensity at 580 nm. The intensity is relative value with respect to that in the absence of the antigen. (B) Fluorescence spectra of RhG-labeled anti-BGP scFv with excitation at 495nm and titration curve for the fluorescence intensity at 527 nm. (C) Fluorescence spectra of double-labeled anti-BGP scFv with excitation at 495 nm, and titration curve for the fluorescence intensity ratio at 527 nm and 580 nm. (D) Fluorescence spectra of double-labeled anti-BGP scFv with excitation at 550 nm, and titration curve for the fluorescence intensity ratio at 580nm. Fluorescence intensities and ratios were expressed as mean ± standard error (n = 3). K_d values were determined by curve-fitting.

(A) TAMRA-labeled anti-bisphenol A scFv

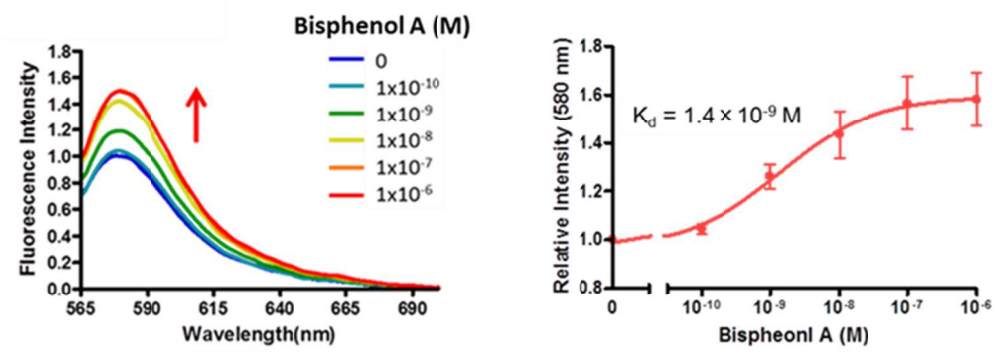

(B) RhG-labeled anti-bisphenol A scFv

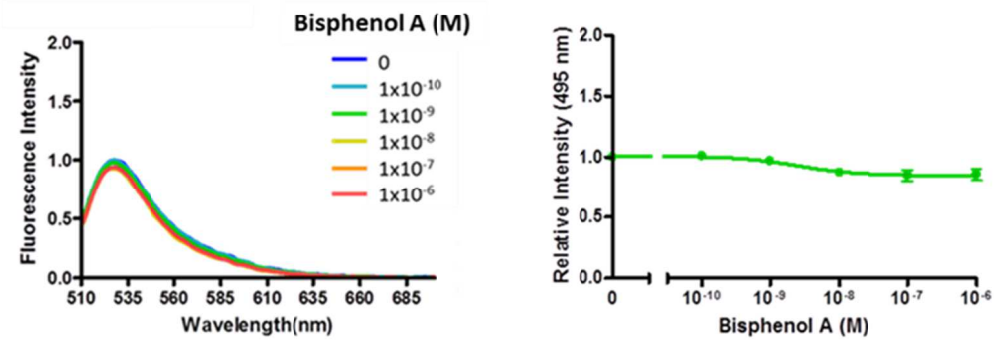

(C) Double-labeled anti-bisphenol A scFv (Ex 495 nm)

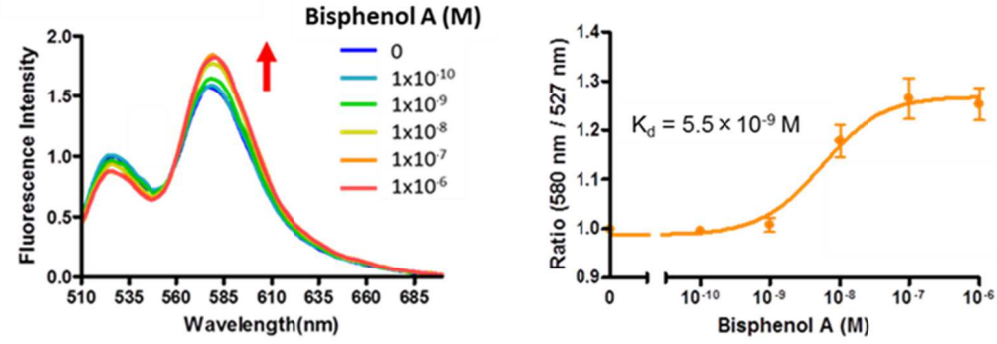

(D) Double-labeled anti-bisphenol A scFv (Ex 550 nm)

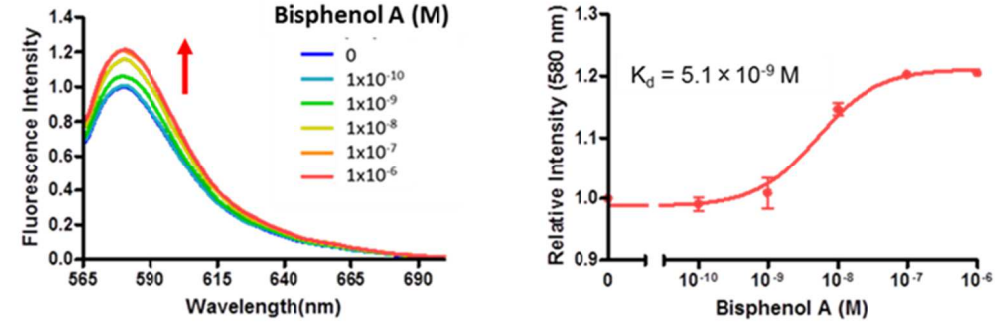

Figure 2.5 Fluorescence measurement of fluorescent-labeled anti-bisphenol A scFvs. (A) Fluorescence spectra of TAMRA-labeled anti-bisphenol A scFv with excitation at 550 nm in the presence and absence of bisphenol A, and titration curve for the fluorescence intensity at 580 nm. The intensity is relative value with respect to that in the absence of the antigen. (B) Fluorescence spectra of RhG-labeled anti-bisphenol A scFv with excitation at 495nm and titration curve for the fluorescence intensity at 527 nm. (C) Fluorescence spectra of double-labeled anti-bisphenol A scFv with excitation at 495 nm, and titration curve for the fluorescence intensity ratio at 527 nm and 580 nm. (D) Fluorescence spectra of double-labeled anti-bisphenol A scFv with excitation at 550 nm, and titration curve for the fluorescence intensity ratio at 580nm. Fluorescence intensities and ratios were expressed as mean ± standard error (n = 3). K_d values were determined by curve-fitting.

3

Fluorescence ratio detection of antigens using double-labeled scFvs with various fluorophore pairs

3.1 Introduction

In Chapter 2, synthesis of double-labeled scFvs and ratiometric detection of antigens by combination with FRET and antigen-dependent fluorescence quenching was investigated. Double-labeled scFvs were synthesized by incorporating tetramethylrhodamine (TAMRA) as a FRET acceptor and Rhodamine Green (RhG) as a FRET donor into N-terminus and C-terminus of scFvs, respectively using nonnatural amino acid mutagenesis in a cell-free translation system.[1] The double-labeled scFvs successfully detected antigens, bone gla protein (BGP) and bisphenol A, in a ratiometric manner (Fig. 3.1A). The fluorescence ratio change was different depending on the type of antigens. Anti-BGP scFv showed 3.8-fold ratio change upon the antigen-binding, while anti-bisphenol A showed only 1.3-fold.

Through the development of double-labeled scFvs with RhG and TAMRA, two problems to be solved appeared. First, in the case of anti-bisphenol A scFv, low ratio change was observed due to low fluorescence intensity change of TAMRA upon the antigen-binding. This might be due to the low fluorescence quenching of TAMRA by Trp residues. Second, when I examined to use anti-cMyc scFv, ratio change was not observed. This may be possibly due to undesirable interaction of RhG with TAMRA-labeled scFv.

To solve these two problems, I explored to use various donor and acceptor fluorophore pairs for double-labeled scFvs. As new acceptor candidates, I explored nonnatural amino acids carrying RhodamineRed (RhRed) and TexasRed fluorophores (Fig. 3.1B). Because RhRed and TexasRed are rhodamine derivatives like TAMRA, they were expected to be quenched by Trp.[2] Next, I incorporated BODIPYFL (BFL)-linked amino acid (BFLAF) in place of RhG-labeled amino acid (RhG-X-AF) (Fig. 3.1B). Because BFLAF has a shorter linker between the amino acid main-chain and the fluorophore, the linker length between C-terminus of scFv and BFL became short. In addition, linker peptide between the C-terminus of scFvs and the donor amino acid was altered from GlyGlyGlyGly to GlyGly to reduce the mobility of the fluorophore.

In this chapter, single- and double-labeled scFvs against bisphenol A and cMyc in addition to BGP were synthesized in a cell-free translation system. Fluorescence

response of these labeled scFvs upon the addition of antigens was measured. The effect of acceptor fluorophores on the antigen-dependent fluorescence quenching and that of donor fluorophores on the interaction between acceptor-labeled scFvs were investigated. According to the findings on these effects, suitable donor and acceptor pairs were utilized to obtain improved double-labeled scFvs showing distinct antigen-dependent fluorescence ratio change.

3.2 Materials and Methods

Materials

BGP peptide (RRFYGPV),C-terminal peptide for human osteocalcin(bone gla protein, BGP) was obtained from Genscript (Piscaway, NJ). Bisphenol A (2,2-Bis(4-hydroxyphenyl)propane) was obtained from Tokyo chemical industry (Tokyo, Japan). c-Myc peptide (EQKLISEEDL) was obtained from Wako (Osaka, Japan). T4 RNA ligase was obtained from Takara Bio (Otsu, Japan). *E.coli* S30 extract for liner template and MagneHis Ni-particles were obtained from Promega (Madison, WI, USA). Zeba desalting column was obtained from Thermo Fisher Scientific (Waltham, MA, USA). Blue prestained protein standard was obtained from New England Biolabs (Ipswitch, MA, USA).

Preparation of aminoacyl-tRNAs

A yeast phenylalanine tRNA containing a four-base anticodon CCCG and lacking two nucleotides (CA) at the 3' end was prepared by PCR and T7 transcription as described previously.[3] The truncated tRNA was ligated with pdCpA acylated with TAMRA-X-AF, RhRed-X-AF, or Texas Red-X-AF[4] in a reaction mixture (90 µL) containing 2.25 nmol of tRNA(-CA), 6.6 nmol of TAMRA-X-AF-pdCpA in DMSO (9 µL), 55 mM HEPES-Na (pH 7.5), 1 mM ATP, 15 mM $MgCl_2$, 3.3 mM DTT, 20 µg/ml BSA, and 108 units of T4 RNA ligase. The reaction mixture was incubated at 4°C for 2 hours. The aminoacylated tRNA was collected by ethanol precipitation. An amber suppressor tRNA derived from *Mycoplasma capricolum* Trp_1 tRNA[5] was prepared and ligated with pdCpA acylated with RhG-X-AF or BFLAF[4] in a similar manner.

Construction of scFv genes

The N-terminus of scFv genes[6] was fused with Prox-tag[4] containing a four base codon (ATG TCT AAA CAA ATC GAA GTA AAC CGGG TCT AAT GAG). The C-terminus of single-labeled scFvs was fused with GlyGlyGlySer and His tag sequence. For double-labeled scFv genes, the C-terminus was fused with

GlyGlyGlyGly, TAG, and His tag sequence. The GlyGlyGlyGly linker was altered by GlyGly for incorporation of BFLAF. The scFv genes were amplified by PCR with a forward primer (ATC GAG ATC TCG ATC CCG) and a reverse primer (TAT AGT TCC TCC TTT CAG), and were transcribed to mRNAs using T7 RNA polymerase as described previously.[3]

Cell-Free Translation

Fluorescent-labeled scFvs were synthesized in an *E. coli* cell-free translation system.[3] The reaction mixture (60 µL) contained 55 mM HEPES-KOH (pH 7.5), 210 mM GluK, 6.9 mM CH_3COONH_4, 12 mM $(CH_3COO)_2Mg$, 1.2 mM ATP, 0.28 mM GTP, 26 mM phosphoenolpyruvate, 1 mM spermidine, 1.9% PEG-8000, 35 µg/ml^{-1} folinic acid, 0.1 mM 19 amino acids except arginine, 0.01 mM arginine, 2 mM oxidized glutathione, 48 µg of mRNA, 2.25 nmol of TAMRA-X-AF-$tRNA_{CCCG}$ and/or 1 nmol of RhG-X-AF-$tRNA_{CUA}$, and 12 µL *E. coli* S30 extract. The reaction mixture was incubated at 37°C for 1 hour. For incorporation of RhRed-X-AF and TexasRed-X-AF, $tRNA_{CCCG}$ aminoacylated with the corresponding amino acids was used in place of TAMRA-X-AF-tRNA. For incorporation of BFLAF, BFLAF-$tRNA_{CUA}$ was used in place of RhG-X-AF-$tRNA_{CUA}$. N-Terminus single-labeled scFvs were synthesized using mRNAs containing CGGG codon at the N-terminal Prox-tag and TAMRA-X-AF-, RhRed-X-AF- or TexasRed-X-AF-$tRNA_{CCCG}$. C-Terminus single-labeled scFvs were synthesized using mRNAs containing UAG codon at the C-terminus and RhG-X-AF- or BFLAF-$tRNA_{CUA}$. After the translation reaction, fluorescent-labeled scFv was purified on Ni-NTA-coated magnetic beads. The translation mixture was diluted by 180 µl of wash buffer (20 mM phosphate buffer, pH 7.5, 0.5 M NaCl, 5 mM imidazole) with 10 M urea and mixed with 24 µL of Ni-NTA beads. After shaking at r.t. for 30 min, the beads were washed once with wash buffer, once with wash buffer with 8 M urea, and thrice with wash buffer. Fluorescent-labeled scFv was eluted with elution buffer (20 mM phosphate buffer, pH 7.5, 0.5 M NaCl, 0.5 M imidazole) at r.t. for 30 min with shaking. To remove remaining free fluorescent amino acids in the elution solution, gel filtration was performed using Zeba desalting column equilibrated with PBST (20 mM phosphate buffer, pH 7.5, 0.5 M NaCl, 0.05% Tween 20).

The products before and after purification were analyzed by 10% SDS-PAGE. The gels were visualized by a fluorescence imager (FMBIO-III; Hitachi Software Engineering) with excitation at 532 nm / emission at 520 nm for RhG and BFL and excitation at 532 nm / emission at 580 nm for TAMRA, RhRed, and TexasRed.

Fluorescence spectral measurements for fluorescent-labeled scFvs

The purified and gel-filtrated fluorescent-labeled scFv solution (60 μL) was diluted with 450 μL of PBST. The resulting solution was divided into 6 tubes (80 μL) and mixed with the serially diluted antigen solutions (20 μL). After incubation at 25°C for 12 hours, fluorescence spectra were measured on Fluorolog-3 (Horiba Jobin-Yvon) at 25°C in a 5×5mm quartz cell. Excitation and emission slit widths were 5.0 nm. For TAMRA-labeled scFvs, fluorescence spectra were measured from 565 nm to 700 nm with excitation at 550 nm. For RhRed-labeled scFvs, fluorescence spectra were measured from 580 nm to 700 nm with excitation at 570 nm. For TexasRed-labeled scFvs, fluorescence spectra were measured from 600 nm to 720 nm with excitation at 550 nm. For single- and double-labeled scFvs with RhG, fluorescence spectra were measured from 510 nm to 700 nm with excitation at 495 nm. For single- and double-labeled scFvs with BFL, fluorescence spectra were measured from 505 nm to 700 nm with excitation at 495 nm. Fluorescence intensity ratio was determined as intensity at 580 nm / intensity at 527 nm for TAMRA and RhG, 580 nm / 510 nm for TAMRA and BFL, 590 nm / 527 nm for RhRed and RhG, and 590 nm / 510 nm for RhRed and BFL. Dissociation constant (K_d) values were calculated by curve-fitting of maximum peak fluorescence intensities or intensity ratios with the use of a sigmoidal dose-response model using GraphPad Prism software (GraphPad, San Diego, CA, USA).

3.3 Results and Discussion

Synthesis and fluorescence measurement of N-terminal fluorescent-labeled scFvs

At first, the antigen-dependent fluorescence intensity change was examined for three types of fluorophores (TAMRA, RhRed, and TexasRed) to explore suitable fluorophores for scFvs against BGP,[7] bisphenol A,[8] and cMyc peptide.[9] These scFv genes were fused with ProX tag containing CGGG codon at the N-terminus, and transcribed to mRNAs using T7 RNA polymerase. Cell-free translation of the mRNAs was performed in the presence of $tRNA_{CCCG}$ aminoacylated with TAMRA-X-AF, RhRed-X-AF and TexasRed-X-AF. The translation products were analyzed by fluorescence imaging of SDS-PAGE. For all of the anti-BGP, bisphenol A, and cMyc scFvs, full-length protein bands showing red fluorescence were observed (Fig. 3.2), indicating the successful synthesis of the N-terminal single-labeled scFvs. The single-labeled scFvs having His tag at the C-terminus were purified by Ni-NTA beads, followed by gel filtration to remove remaining trace amount of free fluorescent amino acids.

Fluorescence spectra of the single-labeled scFvs were measured in the presence of different concentration of the antigens (Fig 3.3). In the case of anti-BGP scFv, fluorescence intensity increases upon the addition of BGP peptide were 7.5, 2.3 and 1.1-fold for TAMRA, RhRed, and TexasRed, respectively (Fig 3.3A). On the contrary, single-labeled anti-bispenol A scFvs with TAMRA, RhRed and TexasRed showed 1.5, 2.1 and 1.04-fold increases upon the addition of bispenol A, respectively (Fig 3.3B). These results suggest that RhRed improves the fluorescence response upon the antigen-binding for anti-bisphenol A scFv, while TAMRA is suitable for anti-BGP scFv. In the case of anti-cMyc scFv, TAMRA and TexasRed showed almost the same fluorescence intensity increase (1.3 and 1.4-fold) upon the addition of cMyc peptide, although RhRed showed lower intensity change (1.1-fold) (Fig 3.3C).

The dissociation constant (K_d) values for TAMRA-, RhRed, and TexasRed-labeled scFvs were determined by fitting the binding curves to be 4.8×10^{-9}, 3.7×10^{-8} and 7.9×10^{-8} M for anti-BGP scFvs, and 1.7×10^{-9}, 2.4×10^{-8} and 5.1×10^{-10} M for anti-bisphenol A scFvs. Anti-cMyc scFvs did not show saturated fluorescence intensity response, and therefore, K_d values were not determined.

Synthesis and fluorescence measurement of double-labeled anti-bisphenol A scFv

According to the above result, double-labeled anti-bisphenol A scFv with RhRed and RhG at the N- and C-termini, respectively, was synthesized. Anti-bisphenol A scFv gene fused with ProX tag containing CGGG codon at the N-terminus, and with

TAG codon and histidine tag at the C-terminus through Gly_4 peptide linker was prepared, and transcribed to mRNA using T7 RNA polymerase. To decode the CGGG and UAG codons, a frameshift suppressor $tRNA_{CCCG}$ aminoacylated with RhRed-X-AF and an amber suppressor $tRNA_{CUA}$ aminoacylated with RhG-X-AF were prepared.[4] The mRNA was expressed in an *E. coli* cell-free translation system in the presence of the fluorescent aminoacyl-tRNAs.

Fluorescence imaging of SDS-PAGE for the cell-free translation products indicated that full-length scFv showing both red fluorescence of acceptor and green fluorescence of donor was observed in the co-presence of RhRed-X-AF-$tRNA_{CCCG}$ and RhG-X-AF-$tRNA_{CUA}$ (Fig 3.4A). In contrast, no fluorescent band corresponding to the full-length scFv was observed only in presence of RhRed-X-AF-$tRNA_{CCCG}$. A ReRed-labeled band whose mobility was slightly faster than the double-labeled scFv could be identified as a translation product obtained by the termination at the UAG codon. In the presence of RhG-X-AF-$tRNA_{CUA}$, no band was observed due to unsuccessful decoding of the CGGG codon at the N-terminus. These results indicated that the double-labeled scFv with RhRed and RhG at the N- and C-termini, respectively, was successfully synthesized in the co-presence of the two fluorescent aminoacyl-tRNAs. The double-labeled scFv was purified by Ni-NTA beads and gel filtration.

Fluorescence spectra of the double-labeled anti-bisphenol A scFv having RhRed and RhG at N- and C-termini, respectively, was measured with excitation at 495 nm and 570 nm (Fig 3.5A). In the case of excitation at 495 nm, both RhG and RhRed fluorescence was observed, indicating FRET from RhG to RhRed. The fluorescence intensity of RhRed increased upon the addition of bispenol A, while RhG intensity slightly decreased. As results of these fluorescence change, fluorescence ratio (RhRed/RhG) increased to 1.7-fold. This value was significantly larger than that of double-labeled scFv with TAMRA and RhG (1.4-fold). Obviously, this larger ratio change of the RhRed- and RhG-double-labeled scFv was due to larger intensity change of RhRed. K_d value of the double-labeled scFv with RhRed and RhG (2.2×10^{-8} M) was comparable to that of the single-labeled RhRed-scFv (2.4×10^{-8} M), suggesting that the C-terminal RhG gave no effect on the antigen-binding.

Under the excitation at 570 nm for the double-labeled scFv, fluorescence intensity increased to 1.8-fold (Fig 3.5B). This change was lower than that of the single-labeled RhRed-scFv (2.1-fold). It may be reasoned that undesirable interaction between donor and acceptor fluorophores affects the fluorescence quenching and recovery of RhRed.

Synthesis and fluorescence measurement of double-labeled anti-cMyc scFvs

Double-labeled anti-cMyc scFv was synthesized by introducing TAMRA and RhG at the N- and C-termini, respectively (Fig. 3.6A). Fluorescence image of SDS-PAGE indicated that the double-labeled anti-cMyc scFv was successfully synthesized in the co-presence of TAMRA-X-AF-tRNA$_{CCCG}$ and RhG-X-AF-tRNA$_{CUA}$ (Fig. 3.4B) as in the case of anti-bisphenol A scFv. Fluorescence spectra of the double-labeled scFv with TAMRA and RhG was measured with excitation at 495 nm. Unexpectedly, the double-labeled scFv showed increase in both TAMRA and RhG fluorescence and irregular change in fluorescence ratio upon the addition of cMyc peptide (Fig 3.6B). Under the excitation at 550 nm for the double-labeled scFv, fluorescence intensity increased to 1.2-fold (Fig. 3.6C), which was lower than that of single-labeled TAMRA-scFv (1.3-fold). This result may be due to undesirable interaction of RhG with scFv and TAMRA.

To reduce the interaction of the donor fluorophore with scFv and the acceptor fluorophore, the use of BFLAF, which has a shorter linker between the amino acid main-chain and fluorophore than RhG-X-AF, was explored (Fig. 3.6A). In addition, the linker peptide between the C-terminus of scFv and the donor fluorophore was altered from Gly_4 to Gly_2. The newly-designed double-labeled scFv was synthesized using a mRNA containing Gly_2 linker between the C-terminus of scFv and UAG codon in the co-presence of TAMRA-X-AF-tRNA$_{CCCG}$ and BFLAF-tRNA$_{CUA}$. Fluorescence image of SDS-PAGE indicated that the double-labeled anti-cMyc scFv with TAMRA and BFL was successfully obtained (Fig. 3.4B).

Fluorescence spectra of the double-labeled anti-cMyc scFv with TAMRA and BFL was measured with excitation at 495 nm. The double-labeled scFv showed significant increase in TAMRA fluorescence with slight increase in BFL fluorescence upon the addition of cMyc peptide (Fig. 3.6D). As results of these changes, fluorescence ratio increased to 1.45-fold. Under the excitation at 550 nm, fluorescence intensity increased to 1.7-fold (Fig. 3.6E), while the single-labeled TAMRA-scFv showed 1.3-fold increase. These results suggest that the linker length for the C-terminal donor fluorophore is important to reduce undesirable interaction of the donor and generate effective double-labeled scFvs.

Synthesis and fluorescence measurement of double-labeled anti-bisphenol A scFv with RhRed and BFL

To examine the possibility that the shorter linker of the C-terminal donor is effective to other scFvs, double-labeled anti-bisphenol A scFv with N-terminal TAMRA and

C-terminal BFL through Gly_2 linker was synthesized in a similar manner to anti-cMyc scFv (Fig. 3.4A). Fluorescence spectra of the double-labeled anti-bisphenol A scFv showed considerable increase in RhRed fluorescence with slight decrease in BFL fluorescence upon the addition of bisphenol A (Fig 3.7A). The fluorescence ratio increased to 2.1-fold, which was larger than that of the double-labeled scFv with RhRed and RhG. Under the excitation at 570nm, fluorescence intensity increased to 2.0-fold (Fig. 3.7B), which was larger than that of the RhG-containing double-labeled scFv and comparable to that of single-labeled RhRed-scFv. These results may be possibly because that undesirable interaction between RhRed and RhG is removed by using the shorter linker between the scFv and the donor fluorophore.

The K_d value obtained from the fluorescence ratio change was 2.4×10^{-8} M, which was comparable to those of RhG-containing double-labeled scFv (2.2×10^{-8} M) and single-labeled RhRed-scFv (2.2×10^{-8} M). This suggests that the C-terminal BFL also did not affect the antigen-binding activity.

3.4 Conclusion

I explored to use various donor and acceptor fluorophore pairs for fluorescence ratio detection of antigens using double-labeled scFvs. By using RhRed as an acceptor fluorophore, the antigen-dependent fluorescence intensity change of anti-bisphenol A scFv was significantly improved. Moreover, fluorescence ratio change of double-labeled anti-bisphenol A scFv with RhRed and RhG was improved compared to TAMRA-containing double-labeled scFv. For anti-cMyc scFv, the use of BFL and shorter linker between the C-terminus of scFv and the donor fluorophore gave expected fluorescence ratio change while the double-labeled scFv with TAMRA and RhG did not. The anti-bisphenol A scFv with RhRed and BFL also showed improved fluorescence ratio change. These results suggest that the selection of donor and acceptor fluorophore pairs and linker length for the C-terminal donor fluorophore is important for effective fluorescence ratio change. Up to now several fluorophores showing large fluorescence intensity change upon the antigen-binding were reported other than TAMRA and RhRed.[10] Because there are other acceptor candidates that can be quenched by Trp residue, further alteration of the acceptor fluorophore will be valuable to improve the antigen-dependent fluorescence ratio change. It has been reported that the incorporation of fluorophores into flexible linkers of scFvs was also available for antigen-dependent fluorescence quenching.[11] Therefore, alteration of the incorporation position of donor fluorophore, in addition to further alteration of linker length between scFv and donor fluorophore, may be available to reduce the undesirable interaction of donor fluorophore with scFv and/or acceptor fluorophore.

The double-labeled scFvs will be useful for various applications such as diagnostic analysis and fluorescence ratio imaging. The improvement of their fluorescence ratio change will enhance the impact of the present strategy, and contribute to practical applications of the double-labeled scFvs.

References

1 Yoshikoshi, K., Watanabe, T. Hohsaka, T. *submitted*.

2 N. Marmé, J-P. Knemeyer, M. Sauer, J. Wolfrum, *Bioconjugate Chem.* **2003,** *14, 1133-1139*

3 T. Hohsaka, D. Kajihara, Y. Ashizuka, H. Murakami, M. Sisido, *J. Am. Chem. Soc.* **1999,** *121*, 34-40.

4 R. Abe, K. Shiraga, S. Ebisu, H. Takagi, T. Hohsaka, *J. Biosci. Bioeng.* **2010,** *110*, 32-38.

5 I. L. Medintz, J. R. Deschamps, *Curr. Opin. Biotechnol.* **2006,** *17*, 17-27.

6 R. Abe, H. Ohashi, I. Iijima, M. Ihara, H. Takagi, T. Hohsaka, H. Ueda, *J. Am. Chem. Soc.* **2011,** *133*, 17386-17394.

7 S-L Lim, H. Ichinose, T. Shinoda, H. Ueda, *Anal. Chem.* **2007,** *79, 6193-6200*

8 K. Nishi, M. Takai, K. Morimune, H. Ohkawa, *Biosci. Biotechnol Biochem.* **2003,** *67, 1358-1367*

9 N. Krauss, H. Wessner, K. Welfie, H. Welfie, C. Scholz, M. Seifert, K. Zubow, J. Aÿ, M. Hahn, P. Scheerer, A. Skerra, W. Höhne, *Proteins.* **2008,** *73, 552-565*

10 H-J. Jeong, Y. Ohmuro-Matsuyama, H. Ohashi, F. Ohsawa, Y. Tatsu, M. Inagaki, H. Ueda, *Biosens.Bioelectron.* **2013,** *40, 17-23.*

11 H-J Jeong, H. Ueda, *Sensors.* **2014**, *14, 13285-13297*

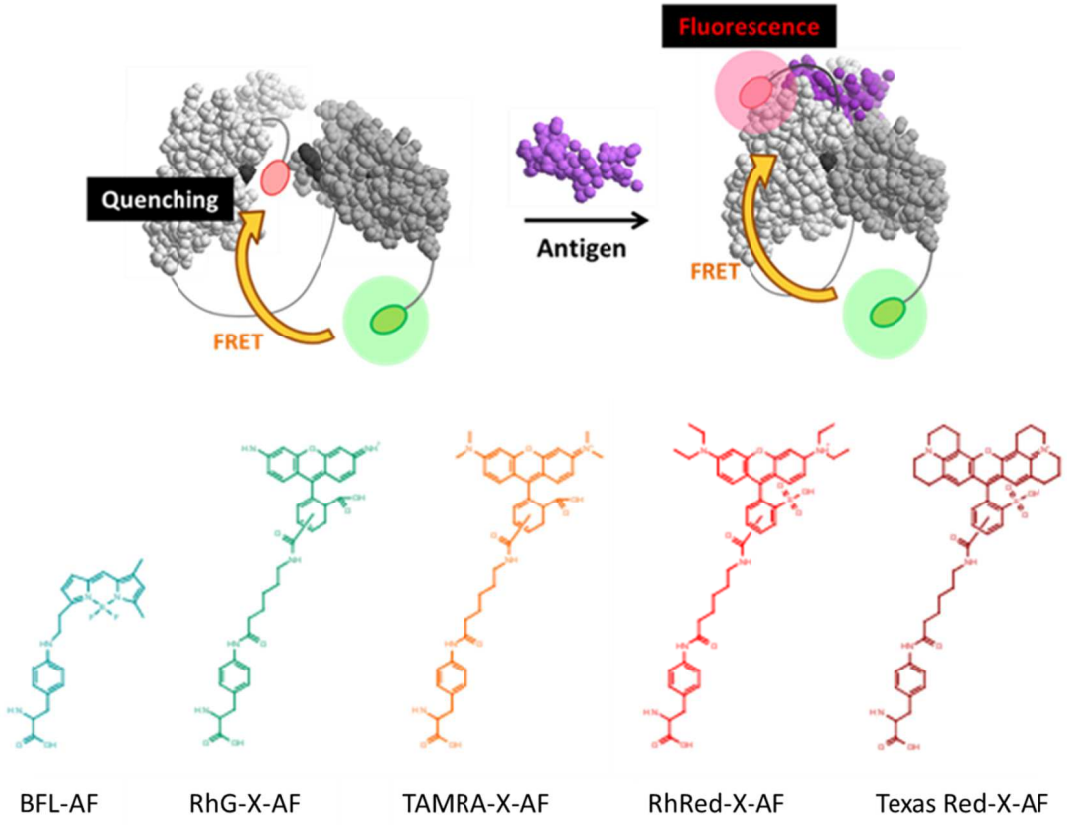

Figure 3.1 (A) Schematic illustration of double-labeled scFv that allows fluorescence ratio detection of antigen by combination with FRET and fluorescence quenching. (B) Structure of fluorescent-labeled nonnatural amino acids used in this study.

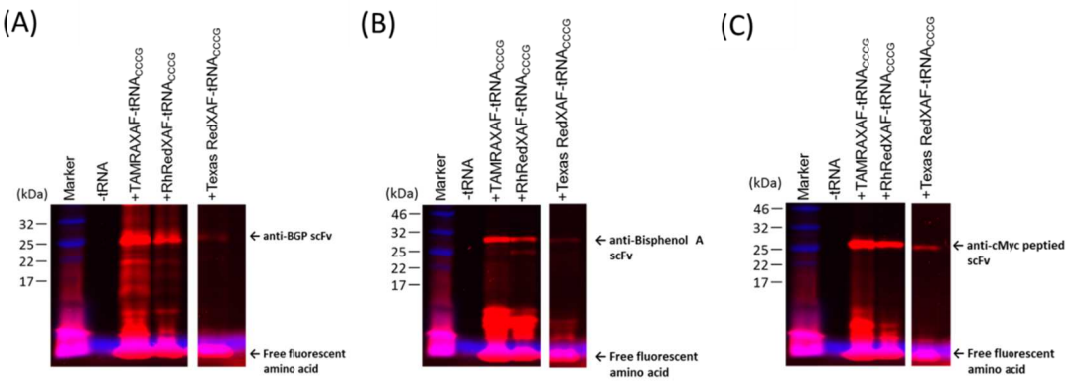

Figure 3.2 Fluorescence imaging of SDS-PAGE for the expression of single-labeled scFvs in the presence of TAMRA-X-AF-, RhRed-X-AF- and TexasRed-X-AF-tRNA$_{CCCG}$ in a cell-free translation system. (A) Anti-BGP scFvs. (B) Anti-bisphenol A scFvs. (C) Anti-cMyc scFvs.

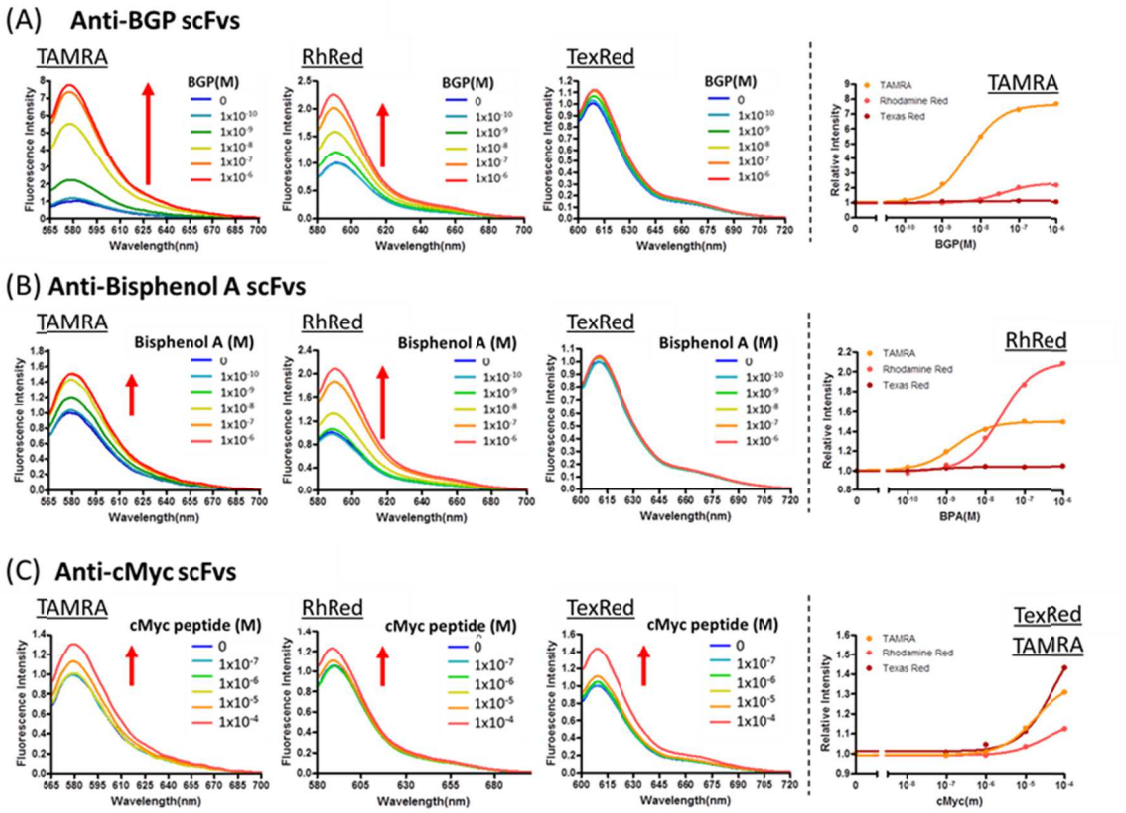

Figure 3.3 Fluorescence measurement of single-labeled scFvs with TAMRA, RhRed, and TexasRed in the presence and absence of antigens. (A) Fluorescence spectra of anti-BGP scFvs. Excitation wavelength is 550, 570, and 600 nm for TAMRA, RhRed, and TexasRed, respectively. Titration curves were obtained from the fluorescence intensities at 580, 595, and 620 nm for TAMRA, RhRed and TexasRed, respectively. The intensity is relative value with respect to that in the absence of the antigen. (B) Fluorescence spectra and titration curves of single-labeled anti-bisphenol A scFvs. (C) Fluorescence spectra and titration curves of single-labeled anti-cMyc scFvs.

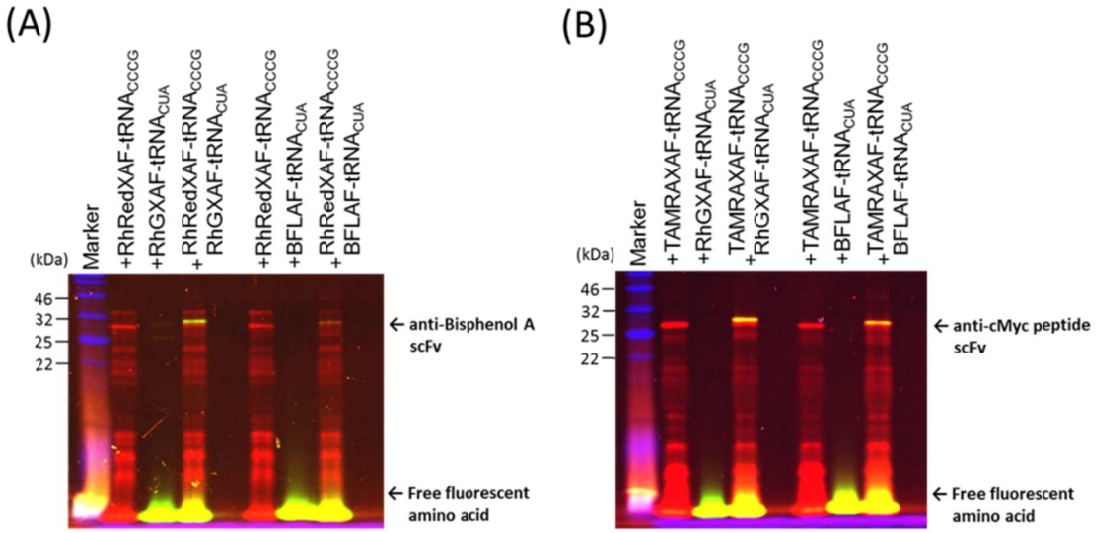

Figure 3.4 Fluorescence image of SDS-PAGE for the expression of double-labeled scFvs in a cell-free translation system. (A) Double-labeled anti-Bisphenol A scFvs expressed in the presence of RhRed-X-AF-tRNA$_{CCCG}$ and RhG-X-AF- or BFLAF-tRNA$_{CUA}$. (B) Double-labeled anti-cMyc scFvs expressed in the presence of TAMRA-X-tRNA$_{CCCG}$ and RhG-X-AF- or BFLAF-tRNA$_{CUA}$.

(A) RhRed-X-scFv(Bisphenol A)-GGGG-X-RhG (Ex 495nm)

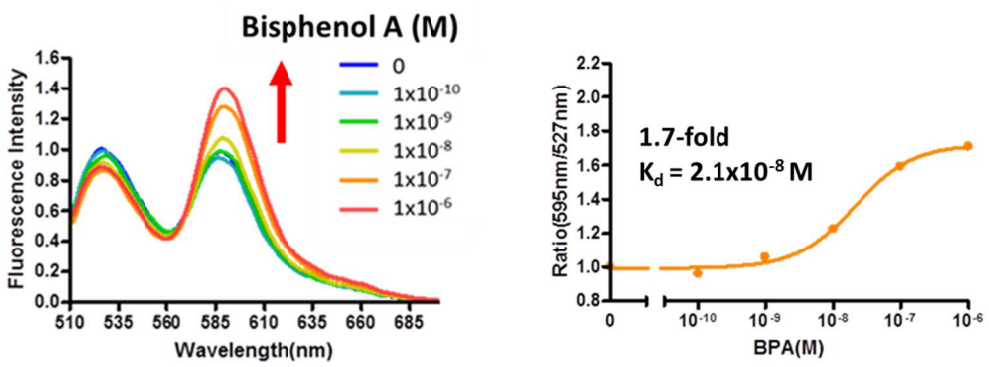

(B) RhRed-X-scFv(Bisphenol A)-GGGG-X-RhG (Ex 570nm)

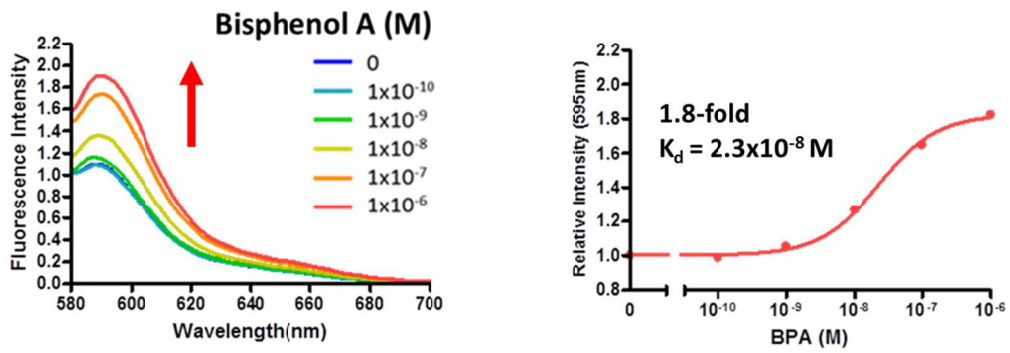

Figure 3.5 Fluorescence measurement of double-labeled anti-bisphenol A scFv with RhRed and RhG in the presence and absence of bisphenol A.
(A) Fluorescence spectra of double-labeled anti-bisphenol A scFv with RhRed and RhG with excitation at 495 nm, and titration curve for the fluorescence intensity ratio at 595 nm and 527 nm. (B) Fluorescence spectra with excitation at 570 nm, and titration curve for the fluorescence intensity ratio at 595 nm.

(A)

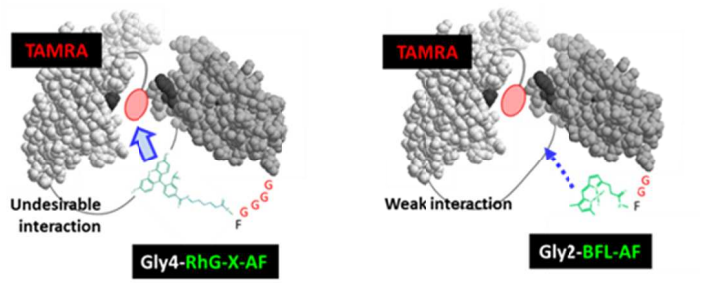

(B) TAMRA-X-scFv(cMyc peptide)-GGGG-X-RhG (Ex 495nm)

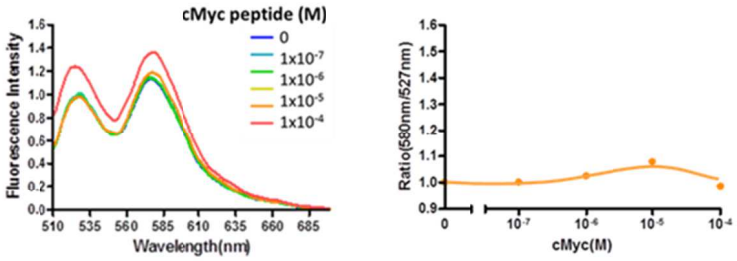

(C) TAMRA-X-scFv(cMyc peptide)-GGGG-X-RhG (Ex 550nm)

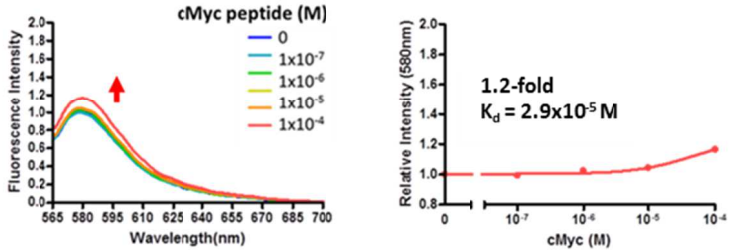

(D) TAMRA-X-scFv(cMyc peptide)-GG-BFL (Ex 495nm)

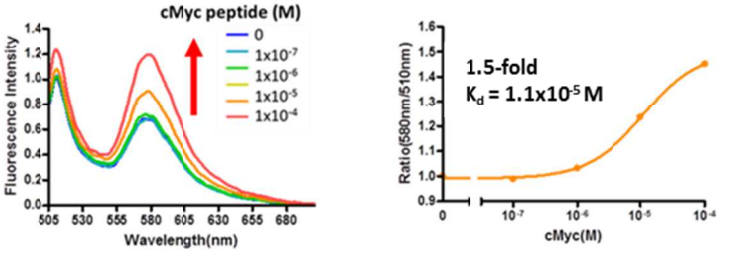

(E) TAMRA-X-scFv(cMyc peptide)-GG-BFL (Ex 550nm)

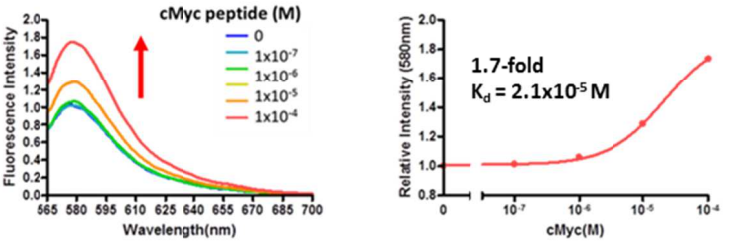

Figure 3.6 Fluorescence measurement of double-labeled anti-cMyc scFvs in the presence and absence of cMyc peptide.
(A) Illustration of double-labeled scFv with TAMRA at the N-terminus and RhG or BFL at the C-terminus. RhG may interact with scFv and TAMRA. BFL with shorter linker reduces this undesirable interaction. (B) Fluorescence spectra of double-labeled anti-cMyc scFv with TAMRA and RhG with excitation at 495 nm, and titration curve for the fluorescence intensity ratio at 580 nm and 527 nm. (C) Fluorescence spectra with excitation at 550 nm, and titration curve for the fluorescence intensity ratio at 580 nm. (D) Fluorescence spectra of double-labeled anti-cMyc scFv with RhRed and BFL with excitation at 495 nm, and titration curve for the fluorescence intensity ratio at 595 nm and 510 nm. (E) Fluorescence spectra with excitation at 550 nm, and titration curve for the fluorescence intensity ratio at 580 nm.

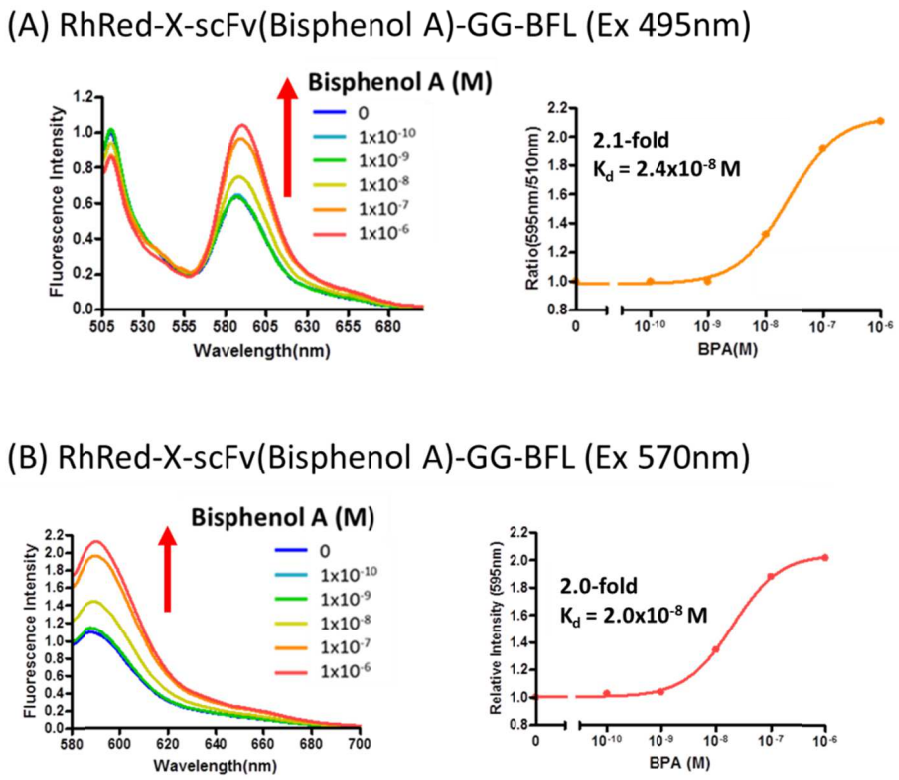

Figure 3.7 Fluorescence measurement of anti-bisphenol A scFv with RhRed and BFL in the presence and absence of bisphenol A.

(A) Fluorescence spectra of double-labeled anti-bisphenol A scFv with excitation at 495 nm, and titration curve for the fluorescence intensity ratio at 595 nm and 510 nm. (B) Fluorescence spectra with excitation at 570 nm, and titration curve for the fluorescence intensity ratio at 595 nm.

4

Fluorescence ratiometric detection of antigens using environment-sensitive probe-labeled scFvs

4.1 Introduction

Protein-based biosensors for various biomolecules have been developed for basic researches on life science, diagnosis of diseases, and environmental monitoring, etc. Among them, antibody-based biosensors (immunosensors) are promising due to high specificity and sensitivity of antibodies. However, commonly used immuneassays like enzyme-linked immunosorbent assay (ELISA) require several rounds of incubation and washing steps, which is difficult to be applied to point of care detection. To solve this issue, various reagentless fluorescent immunoassays have been developed.

First strategy for the reagentless fluorescent immunoassay is the use of antibodies labeled with FRET pairs of two different fluorophores. Distance change between the two fluorophores induced by the antigen-binding causes FRET change. However, the applications of this strategy have been limited[1-4].

Second strategy is the use of N-terminal fluorescent-labeled single-chain antibody variable fragment (scFv) derivatives (Quenchbody).[5,6] The fluorescent-labeled scFvs with fluorophores such as TAMRA and RhodamineRed exhibit fluorescence intensity change depending on the antigen-binding. In the absence of antigen, the fluorophore becomes in close proximity to hydrophobic interface between VH and VL domains and is quenched by conserved Trp residues on the interface. This fluorescence quenching is canceled upon the antigen-binding due to tight interaction between VH and VL domains and removal of the fluorophore from the Trp residues. This principle allows to detect various antigens quantitatively. However, some fluorescent-labeled scFvs does not show fluorescence intensity change because quenching by Trp residue is not enough.

On the other hand, reagentless fluorescent immunoassays using polar-sensitive fluorescent probes have been developed. In this strategy, polar-sensitive probe, IANBD, was attached to complementary determining region (CDR) of anti-hen egg white lysozyme scFv, which showed fluorescence change upon the antigen-binding.[7]

Alternatively, antibody mimic-based methods by using fibronectin type III domain[8] and Ankyrin repeat proteins[9] selected from combinatorial libraries have been reported. The fibronectin type III domain labeled with polar-sensitive probe, merocyanine, and the Ankyrin repeat proteins labeled with IANBD near the

antigen-binding site showed fluorescence change depending on the antigen-binding. Site-specific labeling with polar-sensitive probes and polarity change upon the antigen-binding are essential for these antibody mimics-based biosensors. However, selection of antibody mimics and optimization of the labeling site of polar-sensitive probes require laborious and time consuming steps.

Here, I applied an environment-sensitive fluorescent probe, 5-(dimethylamino)naphthalene-1-sulfonyl group (Dansyl), to the Quenchbody strategy. Dnasyl-labeled scFvs were synthesized by incorporating Dansyl-linked aminophenylalanine (Dansyl-X-AF) into the N-terminus of scFvs. The site-specific incorporation of Dansyl-X-AF was achieved by nonnatural amino acid mutagenesis using an amber codon UAG.[5] Because the maximum wavelength of Dansyl fluorescence shifts depending on polarity changes,[10,11] Dansyl-labeled scFvs can detect antigens as a result of fluorescence wavelength shift in addition of fluorescence intensity change. This allows ratiometric detection of antigens without using FRET donor and acceptor pairs.

Figure 4.1 illustrates two possible mechanisms of fluorescence ratio change of Dansyl-labeled scFvs upon the antigen-binding. In the first possible mechanism (Fig. 4.1A), Dansyl is located at the hydrophobic interface of scFv in the absence of antigen, and emits blue-shifted fluorescence. In the presence of antigen, however, Dansyl is released from the hydrophobic interface due to tight interaction of V_H and V_L domains, and emits red-shifted fluorescence. In the second possible mechanism (Fig. 4.1B), Dansyl is located at the hydrophobic region but exposed to water molecules in the absence of antigen, and emits red-shifted fluorescence. In the presence of antigen, the complex formation of VH, VL, and antigen removes the solvents and generate any hydrophobic region around the antigen-binding site, and as a result, Dansyl emits blue-shifted fluorescence. Because the fluorescence change of Dansyl is based on different mechanisms with previously developed Quenchbodies, this strategy is expected to be available for scFvs that show no or small fluorescence intensity change upon the antigen-binding.

4.2 Materials and Methods

Materials

Dansyl-X-succinimide ester was obtained from Molecular Probes. BGP peptide (RRFYGPV), C-terminal peptide for human osteocalcin (bone gla protein, BGP) and EGF Receptor substrate 2 (Phospho-Tyr[5]) (NANE-pTyr-LIPQQG) were obtained from Genscript (Piscaway, NJ). Bisphenol A (2,2-Bis(4-hydroxyphenyl) propane) was obtained from Tokyo chemical industry (Tokyo, Japan). c-Myc peptide (EQKLISEEDL) was obtained from Wako. T4 RNA ligase was obtained from Takara Bio (Otsu, Japan). *E.coli* S30 extract for liner template and MagneHis Ni-particles were obtained from Promega (Madison, WI, USA). Zeba desalting column was obtained from Thermo Fisher Scientific (Waltham, MA, USA). Blue prestained protein standard was obtained from New England Biolabs (Ipswitch, MA, USA). Anti-His tag monoclonal antibody was obtained from MBL (Nagoya, Japan).

Preparation of Aminoacyl tRNAs

An aminoacylated dinucleotide, Dansyl-X-AF-pdCpA, was synthesized using Dansyl-X-succinimide ester and aminopehnylalanine-pdCpA. An amber suppressor tRNA derived from *Mycoplasma capricolum* Trp_1 tRNA containing an CUA anticodon and lacking two nucleotides (CA) at the 3' end[12] was prepared by PCR and T7 transcription as described previously.[13] The truncated tRNA was ligated with Dansyl-X-AF-pdCpA in a reaction mixture (80 µL) containing 2.25 nmol of tRNA(-CA), 6.6 nmol of Dansyl-X-AF-pdCpA in DMSO (8 µL), 55 mM HEPES-Na (pH 7.5), 1 mM ATP, 15 mM $MgCl_2$, 3.3 mM DTT, 20 µg/ml BSA, and 108 units of T4 RNA ligase. The reaction mixture was incubated at 4°C for 2 hours. The aminoacylated tRNA was collected by ethanol precipitation.

Construction of scFv genes

The N-terminus of scFv genes against BGP. bisphenol A, and cMyc peptide[5] was fused with Prox-tag[15] containing an amber codon (ATG TCT AAA CAA ATC GAA GTA AAC TAG TCT AAT GAG). The C-terminus of these scFvs was fused with GlyGlyGlySer and His tag sequence. In the case of anti-phosphotyrosine scFv, the N-terminus was fused with Prox-tag without TAG codon (ATG TCT AAA CAA ATC GAA GTA AAC TCT TCT AAT GAG) and the C-terminus was fused with GlyGlyGly, TAG codon, and His tag sequence. The scFv genes were amplified by PCR with a forward primer (ATC GAG ATC TCG ATC CCG) and a reverse primer (TAT AGT TCC TCC TTT CAG), and were transcribed to mRNAs using T7 RNA polymerase as

described previously.[13]

Cell-Free Translation

Dansyl-labeled scFvs were synthesized in an *E. coli* cell-free translation system.[13] The reaction mixture (120 μL) contained 55 mM HEPES-KOH (pH 7.5), 210 mM GluK, 6.9 mM CH_3COONH_4, 12 mM $(CH_3COO)_2Mg$, 1.2 mM ATP, 0.28 mM GTP, 26 mM phosphoenolpyruvate, 1 mM spermidine, 1.9% PEG-8000, 35 μg/ml folinic acid, 0.1 mM 20 amino acids, 2 mM oxidized glutathione, 96 μg of mRNA, 4 nmol of Dansyl-X-AF-$tRNA_{CUA}$, and 24 μL *E. coli* S30 extract. The reaction mixture was incubated at 37°C for 1 hour. After the translation reaction, Dansyl-labeled scFv was purified on Ni-NTA-coated magnetic beads. The translation mixture was diluted by 360 μL of wash buffer (20 mM phosphate buffer, pH 7.5, 0.5 M NaCl, 5 mM imidazole) containing 10 M urea and mixed with 48 μL of Ni-NTA beads. After shaking at r.t. for 30 min, the beads were washed once with wash buffer, once with wash buffer containing 8 M urea, and thrice with wash buffer. Dansyl-labeled scFv was eluted with elution buffer (20 mM phosphate buffer, pH 7.5, 0.5 M NaCl, 0.5 M imidazole) at r.t. for 30 min with shaking. To remove remaining free Dansyl-X-AF in the elution solution, gel filtration was performed using Zeba desalting column equilibrated with PBS (20 mM phosphate buffer, pH 7.5, 0.5 M NaCl) containing 0.005% Brij-35. The products were analyzed by 10% SDS-PAGE and the gels were visualized by western blotting with anti-His tag antibody.

Fluorescence spectral measurements for Dansyl-labeled scFvs

The purified and gel-filtrated Dansyl-labeled scFv solution (120 μL) was diluted with 390 μL of PBS containing 0.005% Brij-35. The resulting solution was divided into 6 tubes (80 μL) and mixed with the serially diluted antigen solutions. After incubation at 25°C for 12 hours, fluorescence spectra were measured on Fluorolog-3 (Horiba Jobin-Yvon) at 25°C in a 5×5mm quartz cell. Excitation and emission slit widths were 5.0 nm. Fluorescence spectra were measured from 400 nm to 600 nm with excitation at 335 nm. Baseline subtraction was done using fluorescence spectra of PBS containing 0.005% Brij-35. Fluorescence intensity ratio was determined as intensities at 426 nm / 510 nm for anti-BGP scFv, 420 nm / 488 nm for anti-bisphenol A, and 510 nm / 420 nm for anti-cMyc scFv. Dissociation constant (K_d) values were calculated by curve-fitting of maximum peak fluorescence intensities or intensity ratios with the use of a sigmoidal dose-response model using GraphPad Prism software (GraphPad, San Diego, CA, USA).

4.3 Results and Discussion

Synthesis of Dansyl-labeled scFvs by incorporation of Dansyl-X-AF

The antigen-dependent fluorescence intensity change has been observed for four types of scFvs against BGP, bisphenol A, cMyc, and pTyr. These scFvs were used for Dansyl-labeling in this study. The scFv genes were fused with TAG codon-containing sequence at the N-terminus and His tag at the C-terminus (Fig. 4.2A), and transcribed to mRNA. In the case of anti-pTyr, TAG codon was introduced between the scFv gene and His tag at the C-terminus (Fig. 4.2B), because C-terminus TAMRA-labeled anti-pTyr scFv showed larger fluorescence response upon the antigen-binding than N-terminus labeled one. To decode the UAG codon, an amber suppressor $tRNA_{CUA}$ aminoacylated with Dansyl-X-AF was prepared.[15] The mRNAs were expressed in an *E. coli* cell-free translation system in the presence of Dansyl-X-AF-tRNAs (Fig. 4.2A and 4.2B).

The translation products were analyzed by western blotting with anti-His tag antibody (Fig. 4.3). In the presence of Dansyl-X-AF-$tRNA_{CUA}$, protein bands corresponding to the full-length scFvs were observed. In contrast, no band was observed in the absence of $tRNA_{CUA}$. These results indicated that Dansyl-labeled scFvs were successfully synthesized in the presence of Dansyl-X-AF-$tRNA_{CUA}$. Dansyl-labeled scFvs having His tag at the C-terminus were purified by Ni-NTA beads, followed by gel filtration to remove remaining trace amount of free Dansyl-X-AF.

Fluorescence measurements for Dansyl-labeled scFvs

Fluorescence spectra of Dansyl-labeled scFvs were measured in the absence and presence of antigens. In the absence of antigen, Dansyl-labeled anti-BGP scFv showed broad spectra ranging from 400 nm to 600 nm (Fig 4.4A). On the contrary, the addition of antigen increased the fluorescence at around 420 nm and decreased at around 500 nm. The maximum wavelength was shifted from 427 nm to 418 nm. As a result of the wavelength shift, fluorescence ratio (426 nm / 510 nm) increased by 3.0-fold upon the addition of antigen (Fig 4.4A).

Dansyl-labeled anti-bisphenol A scFv showed similar but more distinct fluorescence spectral change (Fig 4.4B) compared with the anti-BGP scFv. In the absence of antigen, Dansyl-labeled anti-bisphenol A scFv showed red-shifted fluorescence with maximum intensity at 490 nm. The addition of antigen remarkably increased the blue-shifted fluorescence at around 420 nm with the decrease in the red-shifted fluorescence. The fluorescence ratio (420 nm / 488 nm)

increased by 4.0-fold (Fig 4.4B).

The fluorescence change observed for anti-BGP and anti-bisphenol A scFvs suggests that Dansyl is located at partially hydrophilic environment in the absence of antigens and moves to hydrophilic environment upon the antigen-binding. As illustrated in Fig. 4.1B, Dansyl may be located at the interface region but exposed to solvents in the absence of antigen. The antigen-binding may decrease the exposed surface of the scFv and Dansyl may be located at any hydrophobic region around the antigen-binding site.

The relatively strong red-shifted fluorescence observed for anti-bisphenol A scFv in the absence of antigen indicates that Dansyl is located at more hydrophilic environment. This may be due that anti-bisphenol A scFv has less hydrophobic region at the VH-VL interface and the antigen-binding site than anti-BGP scFv. The antigen-binding may generate hydrophobic region around the antigen-binding site.

Unlike anti-BGP and anti-bisphenol A scFvs, Dansyl-labeled anti-cMyc scFv showed blue-shifted fluorescence in the absence of antigen (Fig. 4.4C). The addition of antigen slightly decreased the blue-shifted fluorescence at around 420 nm and slightly increased the red-shifted fluorescence at around 500 nm. The fluorescence ratio change (510 nm / 420 nm) upon the addition of antigen was 1.8-fold (Fig 4.4C). The nearly constant blue-shifted fluorescence observed for anti-cMyc scFv suggests that anti-cMyc scFv has hydrophobic region where Dansyl can be located regardless of the absence and presence of antigen. The antigen-binding may affect the hydrophobic region, and as consequence, Dansyl may move to slightly hydrophilic environment.

Dansyl-labeled anti-pTyr scFv showed mainly blue-shifted fluorescence in the absence of antigen (Fig. 4.4D). In the presence of antigen, the blue-shifted fluorescence increased to 2.3-fold without changing the fluorescence spectral shape. As in the case of anti-cMyc scFv, anti-pTyr scFv may have hydrophobic region where Dansyl can be located regardless of the absence and presence of antigen. The antigen-binding may enhance the hydrophobicity of the hydrophobic region and increase the blue-shifted fluorescence of Dansyl.

The dissociation constant (K_d) values were determined by fitting the binding curves to be 1.3×10^{-7} M, 1.5×10^{-8} M, 3.5×10^{-6} M, and 4.6×10^{-6} M for anti-BGP, bisphenol A, cMyc, and pTyr scFvs, respectively. Comparing with TAMRA-labeled scFvs, the incorporation of Dansyl-X-AF somewhat decreased the binding activity of scFvs.

4.4 Conclusion

We synthesized four types of Dansyl-labeled scFvs and measured their fluorescence changes upon the antigen-binding. All four Dansyl-labeled scFvs showed fluorescence intensity and wavelength changes upon the antigen-binding, which demonstrates that the environmental-sensitive fluorescent probe can be available to detect the environmental changes around the antigen-binding site. However, the fluorescence changes are different depending on the types of scFvs. This may be due to different structural features of scFvs, and the present result indicates that Dansyl-labeling is also useful to examine the structural features of various scFvs. Furthermore, Dansyl-labeled scFvs allowed the detection of antigens as fluorescence ratio changes without FRET donor and acceptor pairs. Dansyl-labeled scFvs will be utilized to detect antigens under heterogeneous conditions where the concentration of fluorescent probes is not constant.

References

1 R. Arai, H. Ueda, K. Tsumoto, W. C.Mahoney, I. Kumagai, T. Nagamune, *Protein Eng.* **2000**, *13, 369-376*

2 Y. Ohiro, R. Arai, H. Ueda, T. Nagamune, *Anal. Chem.* **2002**, *74, 5786-5792*

3 T. Pulli, M. Hoyhtya, H. Soderlund, K. Takkinen, *Anal. Chem.* **2005**, *77, 2637-2642*

4 C-I. C, R. Makino, J. Dong, H. Ueda, *Anal. Chem.* **2015**, *86, 3513-3519*

5 R. Abe, H. Ohashi, I. Iijima, M. Ihara, H. Takagi, T. Hohsaka, H. Ueda, *J. Am. Chem. Soc.* **2011,** *133*, 17386-17394.

6 H-J. Jeong, H. Ueda, *Sensors.* **2014,** *14, 13285-13297*

7 M. Renard, L. Belkad, N. Hugo, P. England, D. Altschuh, H. Bedouelle, *J.Mol. Biol.* **2002**, *318, 429-442*

8 A. Gulyani, E. Vitriol, R. Allen, J. Wu, D. Gremyachinskiy, S. Lewis, B. Dewar, L M. Graves, B. K. Kay, B. Kuhlman, T. Elston, Klaus. M. Hahn, *Nat Chem Biol* **2011,** *12, 437-444*

9 E. Brient-Litzler, A. Pluckthun, H. Bedouelle, *Protein Eng Des Sel,* **2010**, *23, 229-241*

10 T. Hohsaka, N. Muranaka, C. Komiyama, K. Matsui, S. Takaura, R. Abe, H. Murakami, M. Sisido, *FEBS Lett,* **2004,** *560, 173-177*

11 G. Loving, B. Imperiali, *J. Am. Chem. Soc.* **2008,** *130, 13630-13638*

12 H. Taira, Y. Matsushita, K. Kojima, K. Shiraga, T. Hohsaka, *Biochem. Biophys. Res. Commun.* **2008,** *374*, 304-308.

13 T. Hohsaka, D. Kajihara, Y. Ashizuka, H. Murakami, M. Sisido, *J. Am. Chem. Soc.* **1999,** *121*, 34-40.

14 R. Abe, K. Shiraga, S. Ebisu, H. Takagi, T. Hohsaka, *J. Biosci. Bioeng.* **2010,** *110*, 32-38.

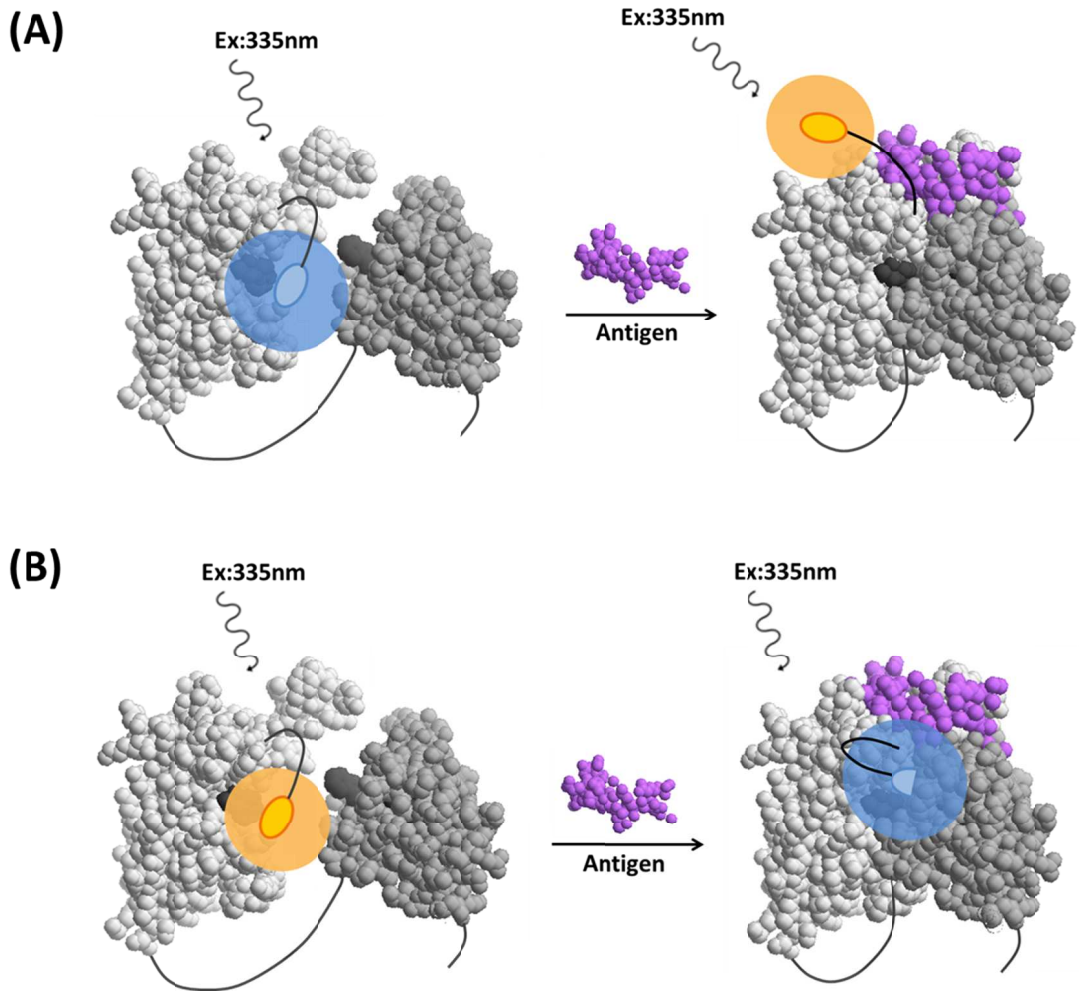

Figure 4.1 Schematic illustration of fluorescence changes of Dansyl-labeled scFv upon the antigen-binding. (A) The first possible mechanism. Dansyl moves from hydrophobic region to hydrophilic solvent upon the antigen-binding. (B) The second possible mechanism. Dansyl moves from relatively hydrophilic region to hydrophobic site upon the antigen-binding.

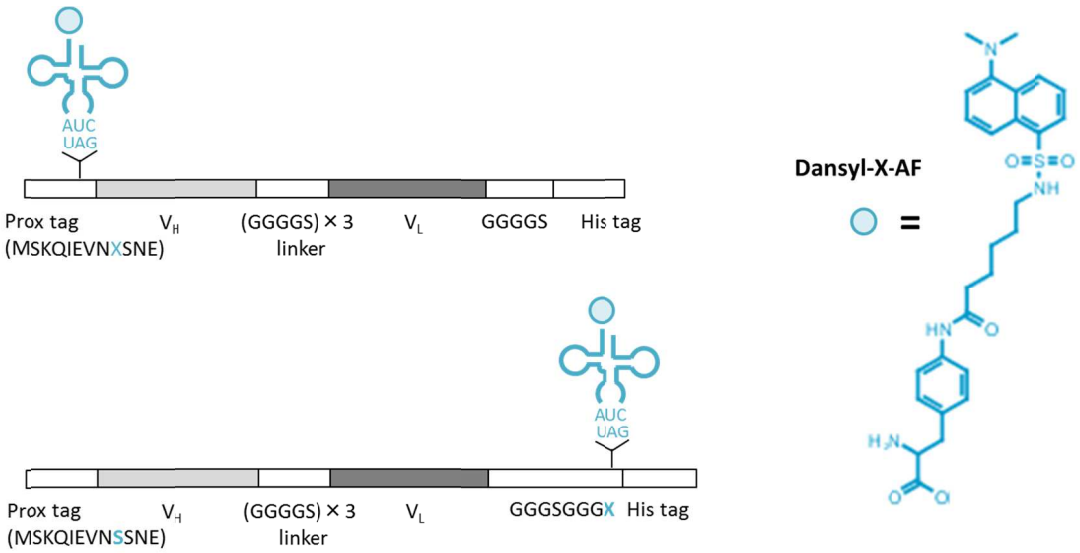

Figure 4.2 Schematic illustration of synthesis of Dansyl-labeled scFvs using an amber codon (UAG) in a cell-free translation system. Dansyl-X-AF is incorporated at the N-terminus for anti-BGP, bisphenol A, and cMyc scFvs (A), and at the C-terminus of anti-pTyr (B).

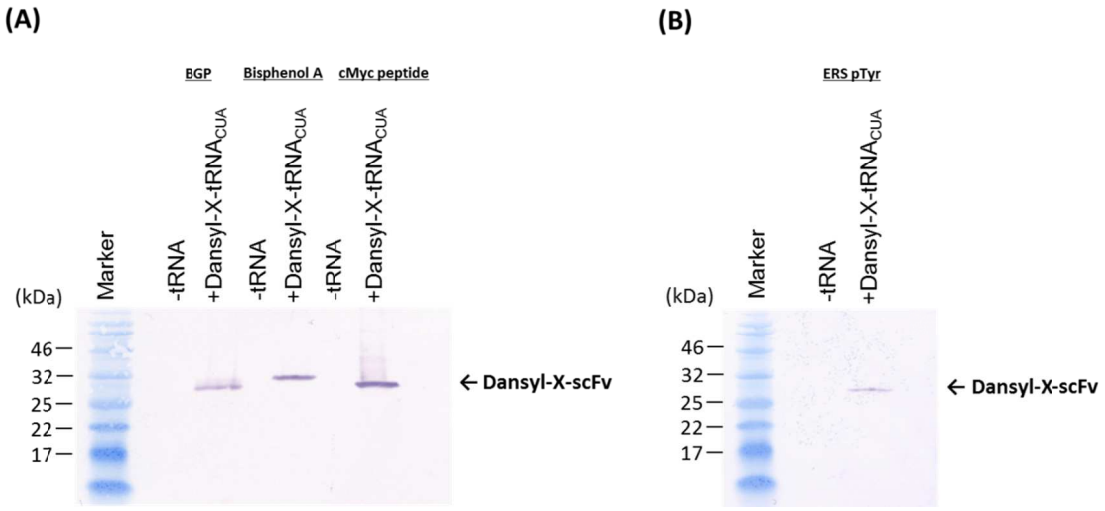

Figure 4.3 Western blotting of SDS-PAGE for the expression of Dansyl-labeled scFvs in the presence of Dansyl-X-tRNA$_{CUA}$ in a cell-free translation system. (A) Dansyl-labeled anti-BGP, bisphenol A and cMyc scFvs (B) Dansyl-labeled anti-pTyr scFv.

(A) Anti-BGP

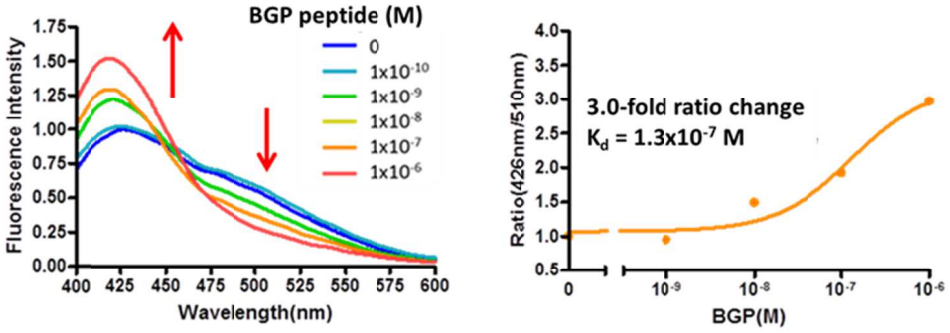

(B) Anti-Bisphenol A

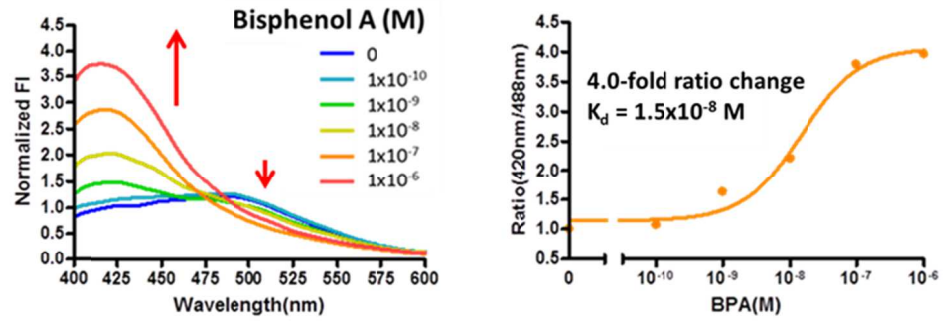

(C) Anti-cMyc

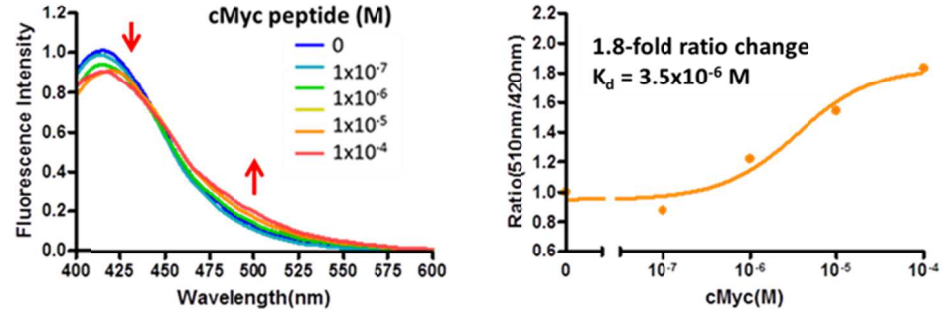

(D) Anti-ERS pTyr

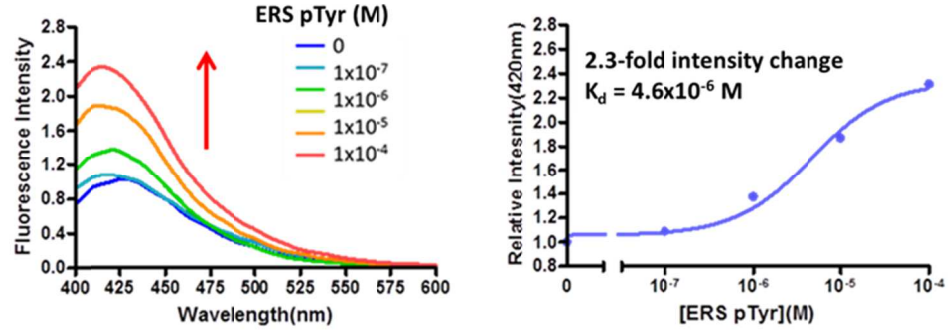

Figure 4.4 Fluorescence measurement of Dansyl-labeled scFvs with excitation at 335 nm in the presence and absence of antigens. (A) Fluorescence spectra of Dansyl-labeled anti-BGP scFv and titration curve for the fluorescence intensity ratio at 426 nm and 510 nm. (B) Fluorescence spectra of Dansyl-labeled anti-bisphenol A scFv and titration curve for the fluorescence intensity ratio at 420 nm and 488 nm. (C) Fluorescence spectra of Dansyl-labeled anti-cMyc scFv and titration curve for the fluorescence intensity ratio at 510 nm and 420 nm. (D) Fluorescence spectra of Dansyl-labeled anti-pTyr scFv and titration curve for the fluorescence intensity ratio at 420nm.

5

Summary and conclusion

In chapter 2, I synthesized double fluorescent-labeled scFvs using non-natural amino acid mutagenesis. TAMRA and RhodamineGreen were incorporated into N- and C-termini of scFvs in response to four-base and amber codons, respectively. I performed fluorescence measurement for double-labeled anti-BGP and anti-bisphenol A scFvs. As a result, fluorescence intensity ratio changes were observed upon the antigen-binding by the combination with FRET and fluorescence quenching. These result suggested that the double-labeled scFvs will be useful as general fluorescence ratio probes for detection of various target molecules.

In chapter 3, I explored acceptor and donor fluorophore pairs and optimized flexible linker length between the donor fluorophore and the C-terminus of scFvs to improve fluorescence ratio changes. As a result of fluorescence measurement for fluorescent-labeled three types of scFvs against BGP, bisphenol A, and cMyc, I found that suitable fluorophores were different depending on the type of scFvs, and RhodamineRed significantly improved the fluorescence response for anti-bisphenol A scFv. Moreover, I revealed that the use of BODIPYFL-linked amino acid with a shorter linker and a shorter peptide linker at the C-terminus of anti-cMyc scFv improved fluorescence ratio change possibly because of decreased undesirable interaction. The shorter linker was also effective for RhodamineRed-labeled anti-bisphenol A scFv. These findings will be valuable for construction of various double-labeled scFvs and their improvement.

In chapter 4, I incorporated Dansyl group as an environment-sensitive fluorescent probe into scFvs and examined fluorescence spectral properties of Dansyl-labeled scFvs. Four types of Dansyl-labeled scFvs against BGP, bisphenol A, cMyc, and pTyr were synthesized using non-natural amino acid mutagenesis. As a result of fluorescence measurements, all four Dansyl-labeled scFvs showed fluorescence spectral changes upon the antigen-binding, This demonstrates that the environment-sensitive fluorescent probe can be applied to monitor environmental changes around the antigen-binding site and to detect antigens in a ratiometric manner. Dansyl-labeling will become an alternative strategy to design and synthesis of scFv-based fluorescent ratio probes.

Over this research, we developed new fluorescence ratio probe to detect target molecules. However, there are drawbacks that are low quantity of the product and high cost the method using cell-free translation system and chemically aminoacyl-tRNA. In addition, it is difficult to express fluorophore-labeled scFv inside cell. Solving these issues will enable us to develop practical diagnostic regent and perform cell imaging, which will contribute to further development of fluorophore-labeled scFv.

Publication list

Double fluorescent-labeled single-chain antibodies showing antigen-dependent fluorescence ratio change. Kensuke Yoshikoshi, Takayoshi Watanabe, Takahiro Hohsaka, *Bull. Chem. Soc. Jpn*,, *in press*.

Fluorescence ratio detection of antigens using double-labeled scFvs with various fluorophore pairs. Kensuke Yoshikoshi, Takahiro Hohsaka, in preparation.

Ratiometric detection of antigens using environment-sensitive probe-labeled scFvs. Kensuke Yoshikoshi, Takahiro Hohsaka, in preparation.

Other Publication

Antibody-Based Fluorescent and Fluorescent Ratiometric Indicators for Detection of Phosphotyrosine. Kim Phuong Hynh Nhat, Takayoshi Watanabe, Kensuke Yoshikoshi, Takahiro Hohsaka, *J. Biosci. Bioeng., in press*.

Acknowledgments

This study was carried out at the School of Materials Science, Japan Advanced Institute of Science and Technology under the supervision of Professor Takahiro Hohsaka. I express my sincere thanks for his kind and long-standing guidance, and encouragement throughout the present study.

I specially acknowledge Dr. Takayoshi Watanabe for his kind technical support and guidance.

I greatly appreciate Dr. Rumi Shiba, Dr. Keisuke Fukunaga, Dr. Dian, Novitasari, Ms. Huynh Nhat Kim Phuong, Mr. Mizuho Fukagawa, Mr. Osamu Toda and all members and graduates of Professor Hohsaka's Laboratory for their kindness and helpful advices.